Kobe University Repository : Kernel

PDF issue: 2024-12-14

A lattice polymerization model and an effective kinetic model for the dynamics of cytoskeletal filaments

古田，忠臣

(Degree)
博士（理学）

(Date of Degree)
2003-09-30

(Date of Publication)
2008-10-16

(Resource Type)
doctoral thesis

(Report Number)
甲2917

(URL)
https://hdl.handle.net/20.500.14094/D1002917

※ 当コンテンツは神戸大学の学術成果です。無断複製・不正使用等を禁じます。著作権法で認められている範囲内で、適切にご利用ください。

KOBE UNIVERSITY

博士論文

A lattice polymerization model and an effective kinetic model for the dynamics of cytoskeletal filaments

(細胞骨格フィラメント・ダイナミクスの
格子重合モデルと有効反応速度論モデル)

平成15年8月

神戸大学大学院自然科学研究科

古田 忠臣

Doctoral thesis

A lattice polymerization model and an effective kinetic model for the dynamics of cytoskeletal filaments

Tadaomi Furuta

Division of Material Functions
Department of Mathematical and Material Science
Graduate School of Science and Technology
Kobe University
Kobe 657-8501, Japan

August 2003

Acknowledgments

First of all, I wish to express my gratitude to my supervisor, Professor Kuniyoshi Ebina for invaluable suggestions, comments, discussions, and instructions. I am also grateful to many colleagues and friends of Kobe University, in particular, Satoshi Ohyama, Koji Sugimoto, Masahiko Ohkubo for fruitful discussions, suggestions and encouragement. Finally, I am thankful to my family for their constant patience and encouragement.

Abstract

In this thesis, I introduce a lattice polymerization model for the dynamics of cytoskeletal filaments including physical ingredients of (a) random motion in space, (b) short range interaction with a threshold length, and (c) internal state dynamics. I also introduce an effective kinetic model for linear polymerization with a threshold length in a finite volume system. Using the lattice model, I simulate the characteristic behavior of a single filament called *dynamic instability* which is a phenomenon repeating slow growth phases and rapid shrinkage phases of a single microtubule length observed *in vivo* and *in vitro*. I calculate the probability distribution functions of short-time mean velocities with different time lags of a single filament in several low concentration in the case of parameters showing the *dynamic instability* and I found that the probability distribution functions have a peak in the positive velocity region which is essentially independent of time lags. I also define a critical concentration balancing the growth and shrinkage. I analyze the length behavior of a single filament in the two limiting cases of a interaction parameter in the lattice polymerization model without internal state variables which are corresponding to the lattice gas model and the diffusion limited aggregation model. As a result, the growth velocity is dependent on the concentration linearly (i.e a diffusive growth) and the shrinkage velocity is almost dependent on the interaction parameter and independent of the concentration. I also found some kind of shifted peak in the length distribution of linear polymers which are longer than the threshold length in the lattice model without the internal state dynamics. To understand the property of this shifted peak, I construct an effective kinetic model with a threshold length in a finite volume system. The effective kinetic model shows a shifted peak of the distribution over the threshold length in each concentration like the shifted peak simulated in the lattice polymerization model. I also found that the average length of filaments in the kinetic model depends on the threshold length exponentially and these peaks relax with time. These suggests that the nucleation is a critical factor to the cellular dynamics. The lattice model and the kinetic model is somewhat artificial but important for the understanding of cellular process and the nature of cytoskeletal subunits.

Contents

1 Introduction **1**

1.1 Motivation 1

1.2 Experimental background of cytoskeletal filaments 2

1.2.1 Cell 2

1.2.2 Cytoskeletal filaments 4

1.3 Theoretical background of cytoskeletal filaments 9

1.3.1 The Oosawa's equilibrium and kinetic theories 9

1.3.2 Kinetic model for the treadmilling 13

1.3.3 Reaction-diffusion model for the dynamic instability 14

1.4 Purpose of the thesis 15

1.5 Structure of the thesis 15

2 A lattice polymerization model **16**

2.1 Essential physical ingredients for the dynamics of cytoskeletal filaments 16

2.2 A lattice polymerization model for the dynamics of cytoskeletal filaments 17

2.3 Measurement of length 19

3 An effective kinetic model **20**

3.1 Polymerization 20

3.2 An Effective Kinetic Model 21

4 Results I: models with threshold length **23**

4.1 Results in the lattice polymerization model without the internal state dynamics 23

4.1.1 Two limiting cases: DLA and LGM in low concentrations . . . 24

4.1.2 Several cases: possible concentrations and detach probabilities 27
4.2 Shifted peak of length distribution in the lattice polymerization model without the internal state dynamics 35
4.2.1 Length distribution of polymers with length l in the effective kinetic model 37
4.2.2 Time evolution of the average length of polymers 40
4.3 Time relaxation of the monomer concentration 41

5 Results II: a model with internal state dynamics 43
5.1 Dynamic instability in the lattice polymerization model 43
5.2 A critical concentration in the lattice polymerization model 44
5.3 Probability distribution function of the short-time average velocity of the length in the lattice polymerization model 45

6 Summary 50

A Two mathematical relations 53

B Law of mass action and Linear response coefficient 54
B.1 Law of mass action 55
B.2 Linear response 55

Chapter 1

Introduction

In this chapter, I state a need for a specified stochastic model for the understanding of the recent phenomena observed *in vivo* and *in vitro*. I briefly review the experimental background of cell and cytoskeleton and the theoretical background of polymerization dynamics for cytoskeletal filaments. And I state the purpose and the structure of the thesis.

1.1 Motivation

Recently the microscopic observation of the dynamics of a single macromolecule such as a large protein or a supramolecule (i.e. a self-assemble chemical aggregate) has become possible *in vivo* (i.e. in a living cell) or *in vitro* (i.e. in a test tube) in many laboratories [1, 2, 3, 4, 5]. Many new features have emerged in the works of many authors (for a review see [6]). To understand the phenomena and their mechanisms, we need more specified models than that of macroscopic thermodynamics or chemical reaction kinetics and we should treat the reaction kinetics more appropriately like Oosawa et al.[7] (in which they discuss the linear and helical polymerizations of macromolecules and treat not only a polymer concentration but also a monomer concentration explicitly (see the subsection 1.3.1)). It is observed that the motions of single macromolecules are rather stochastic and irregular. However they are also energetically controlled and not completely random. On the other hand, these objects are quite large compared to the atomic scale so that the microscopic approach starting from an atomic Hamiltonian is still a formidable task. Therefore we need a new

model, which is essentially stochastic but containing necessary energetics in order to understand the observed dynamical phenomena. Such a new model would build a cross bridge between the protein scale and the cell scale and may be called as a mesoscopic model.

Here I review the experimental background of the cell, in particularly, cytoskeletal filaments briefly.

1.2 Experimental background of cytoskeletal filaments

1.2.1 Cell

The basic unit of life is a biological cell [6]. Among the many events that occur in a living cell, specific chemical transformations provide the cell with usable energy and the molecules needed to form its structure and coordinate its activities. Water is the most abundant molecule in a cell though there exist many small molecules (e.g. ions, sugars, vitamins, fatty acids) and organic macromolecules (e.g. DNA, proteins, polysaccharides). Here if I assume a cell size to be 0.001 cubic mm which is 0.1 mm in the linear dimension (though there are various sizes in cells such as the size exceeds 10 cm in linear scale like the egg of an ostrich) and assume this small box filled up with water. Then there exists about 3×10^{16} water molecules (H_2O) which is derived from the relationships between weight and volume i.e. 1 cm^3 water weighs 1 g and the relationships between the molecular weight and the Avogadro's number i.e. 18 g water corresponds to 6.02×10^{23} molecules. To think of water freezing as one of physical phanomena, this number is too large to simulate freezing using the molecular dynamics method in the present super computer [8] where 512 water molecules are freezed. So the biological cell is not easy to understand the whole instead of its smallness. The biological cell also does not consists of only water (described in the next paragraph) so that it is so complex a world like a jungle. Though there exist some tremendous simulation models like E-Cell which simulate whole cell processes including metabolism, gene expression, etc.[9], the model ignore the spatial effect. I think the spatial effect is important for the cellular processes.

The biological universe consists of two types of cells: *prokaryotic cells*, which lack a defined nucleus and have a simplified internal organization, and *eukaryotic cells*, which have a more complicated internal structure including a defined, membrane-limited nucleus. Here I abstract five major subcellular systems (subsystems) which exist commonly in nearly all the eukaryotic cells. Major five subsystems are as follows: (i) (information) **storage** subsystem consisting of nuclei including DNA, RNA, proteins, ions, water, nuclear membrane, etc., (ii) **boundary** (or interface) subsystem consisting of cell membrane (and cell wall in the case of plant) including Golgi vesicles, ion channels and pumps, ions, water, etc., (iii) **fuel-factory** subsystem of mitochondria including intracellular membranes, proteins, ions, water, etc., (iv) **material-factory** subsystem of the rough and smooth endoplasmic reticula including ribosomes, plasma membranes, ions, water, etc., and (v) **network** subsystem of cytoskeletons and centrosomes including cytoskeletal filaments, their subunit proteins, their associating proteins like motor proteins, ions, water, etc..

Next I describe the functions of above five subsystems. The storage subsystem, (i), preserves genetic information and expresses genes appropriately i.e. synthesizes mRNAs and ships off mRNAs appropriately. And in this subsystem there exists the central dogma of molecular biology that DNA directs the synthesis of RNA, and RNA then directs the synthesis of proteins. However, the one-way flow of information posited by the central dogma (DNA $\rightarrow$ RNA $\rightarrow$ protein) does not reflect the role of proteins in facilitating the information flow. The boundary subsystem, (ii), plays a role as the interface between cellular and external world and in this system Golgi vesicles direct membrane constituents to appropriate places in the cell. The fuel-factory subsystem, (iii), synthesizes ATPs as energy of life and much of the cell's energy metabolism is carried out in this subsystem. The material-factory subsystem,(iv), synthesizes proteins in cooperation with tRNA on the basis of mRNA information from nuclei and also synthesizes lipids. And the network subsystem,(v), devises an important strategy of life, i.e. disperses their subunits in the cytoplasm as electrolyte solution for the cell motility, cell division and morphogenesis. It constructs and destroys "rails" not only for the transport but also for the motion and shape of a cell. The motor proteins walk on these "rails" of cytoskeletal filaments stochastically. I

list some typical motor speeds in Table1.1 (based on [10]).

Motor	Speed *in vivo* [nm/s]	Speed*in vitro* [nm/s]
Myosin II	6,000	8,000
Myosin V	200	250
Cytoplasmic Dynein	-1,100	-1,250
Kinesin	1,800	840

Table 1.1: Motor speeds *in vivo* and *in vitro* A positive speed denotes motion toward the plus (rapidly polymerizing) end of the filament. A negative speed denotes motion toward the minus end. Myosin walks on an actin filament and Dynein and Kinesin walk on a microtubule.

This thesis deals with components of (v) **network** subsystem i.e. cytoskeletal filaments. So I briefly review the cytoskeletal filaments in the next section.

1.2.2 Cytoskeletal filaments

Functions of cytoskeletal filaments

Cytoskeletal filaments are the multi-functional and dynamic objects in the biological cells [6]. There are three major classes of cytoskeletal filaments: **actin filaments** (also called microfilaments), **microtubules**, and **intermediate filaments**. I state the functions of cytoskeletal filaments below briefly. Myosins' walkings on the actin filament make the muscle contraction which is so important in the animals (a myosin is a linear motor protein). Microtubules constitute spindles from two centrosome origins in the process of cell division and constitute cytoskeletal structures to make cellular transport in the other interval from one centrosome origin, where a centrosome itself consists of 9 + 2 structure microtubules: 9 microtubule triplets and 2 microtubule singlets. Motor proteins such as kinesin and dynein walk on the microtubule. Other 9 + 2 microtubules: 9 microtubule doublets and 2 microtubule singlets constitute flagellum and cilia which make the rotating motion by the F_1F_0 protein complex [11]. Microtubules also maintain the function and structure of neurons by lining in parallel in cooperation with microtubule associating proteins (MAPs). Intermediate filaments give elasticity in the biological cells.

Structures of cytoskeletal filaments

The structure of a microtubule is a cylinder consisting of 13 protofilaments[1] , in outer diameter of about 25 nm and in inner diameter of about 18 nm [12]. The structure of an actin filament is double helix consisting of 2 protofilaments in diameter of 8 nm [13]. These structures of two types of cytoskeletal filaments have been analyzed by the technology of the X-ray crystallography in 1970's. The structure of an intermediate filament is quadplex of double helix consisting of 8 protofilaments, in diameter of 10 nm [14] which is like the ether cable of the present computer network. The structure of an intermediate filament has not been determined completely at present. The lengths of these cytoskeletal filaments span the scale from molecular to cellular scale ($\sim 100\mu$m (=0.1 mm)). I summarize the structure of cytoskeletal filaments in Table1.2.

Cytoskeletal filament	Microtubule	Actin filaments	Intermediate filament
Number of Protofilaments	13 (9–17)*	2	8 (6–10)*
Diameter [nm]	25	8	10
Subunit	$\alpha\beta$-tublin dimer	actin monomer	keratin, vimentin, lamin dimers, etc.(called IF proteins)

Table 1.2: Structures of Cytoskeletal Filaments. * The number of protofilaments range in several value depending on their environment.

Structures of subunits of cytoskeletal filaments

The subunits of cytoskeletal filaments are proteins. The subunit of microtubule is a $\alpha\beta$ **tubulin** heterodimer which consists of 8-nm-dumbbell-shape proteins dimerized of slightly-different 4-nm-globule proteins [15]. The subunit of actin filament is an **actin** monomer which is a 5-nm-globule protein [16]. And the subunit of an intermediate filament consists of several protein dimers such as a vimentin dimer, a lamin dimer, a keratin dimer and so on (these are called **IF proteins**), these are helical (i.e. not globular) several-nm proteins. The structures of a tubulin and a actin were analyzed by the cooperations of the technology of the electrocrystallography and the DNA sequencing. The subunit proteins constitute protofilaments (linear filament)

[1] where a protofilament stands for the number of lines which subunits are arranged linearly.

described above. But I state again the number of protofilaments in relation to the growth of a filament by a subunit addition. A microtubule has 13 protofilaments, so the growth of a filament by one tubulin dimer addition is 8 nm / 13 $\sim$ 0.62 nm. An actin filament has 2 protofilaments, so the growth of a filament by one actin addition is 5 nm / 2 = 2.5 nm. And I estimate the growth of a filament by one IF protein as 20 nm / 8 $\sim$ 2 nm.

Hydrolysis in cytoskeletal subunits

Hydrolysis occurs in the subunit proteins of cytoskeletal filaments. The binding nucleotide **GTP** at the β (exchangeable) site of a $\alpha\beta$ tubulin hetero dimer hydrolyze to GDP more frequently in the microtubule than that in a dispersed tubulin dimer. The binding nucleotide **ATP** binding to an actin filament (F-actin) hydrolyze to ADP (G-actin) more frequently than that in an dispersed actin monomer. The head domain of a IF protein belonging to a intermediate filament also hydrolyze more frequently than that in a dispersed IF protein. I speculate that GTP plays a role of information and ATP plays a role of energy in cellular processes.

Four hierarchical structure of proteins

The structure of proteins commonly is described in terms of four hierarchical levels of organization. The *primary structure* of a protein is the linear arrangement, or sequence, of amino acid residues that constitute the polypeptide chain. *Secondary structure* refers to the localized organization of parts of a polypeptide chain, which can assume several different spatial arrangements (so called an α helix, a β sheet, a turn or a random coil). *Tertiary structure*, the next-higher level of structure, refers to the overall conformation of a polypeptide chain, that is, the three-dimensional arrangement of all the amino acids residues. This tertiary structure is stabilized by hydrophobic interactions between the non polar side chains and determines its function. Multimeric proteins contain two or more polypeptide chains, or subunits, held together by non-covalent bonds. *Quaternary structure* describes the number (stoichiometry) and relative positions of the subunits in a multimeric protein.

From the viewpoint of the above hierarchical structure, cytoskeletal filaments are quaternary structures of proteins. Cytoskeletal filaments also called macromolecular

assemblies or *supramolecules* [17]. The understanding of tertiary (three-dimensional) structures of proteins from the primary structures (sequence) is one of the most interesting topic so called *foldings of proteins*. And the understanding of cytoskeletal filaments would lead to the mesoscopic phenomena in cellular processes and also build a cross bridge between the protein scale and the cell scale.

I summarize the structure and properties of cytoskeletal subunits in Table1.3.

Subunit	$\alpha\beta$-tublin dimer	Actin	Keratin, vimentin, lamin, etc.
Shape	dumbbell	globule	double helix
Size of subunit [nm]	8 (=4+4)	5	~ 20
Growth of filament by one subunit addition [nm]	0.61	2.5	~ 2
Molecular mass [kDa]	100 (=50+50)	45	$40 \sim 180$
Hydrolysis	GTP $\rightarrow$ GDP on β	ATP $\rightarrow$ ADP	occurs on the head domain
Nucleotide exchange	GDP $\rightarrow$ GTP on β	ADP $\rightarrow$ ATP	non

Table 1.3: Structure and Properties of cytoskeletal subunits

Polymerizations of cytoskeletal filaments

Polymerizations of cytoskeletal filaments have three major phases: (I) nucleation (lag) phase, (II) growth (polymerizing) phase, and (III) steady-state (equilibrium) phase. In the nucleation phase, (I), assembly and disassembly of cytoskeletal filaments depend on the critical concentration, c_c, of their subunits. Above the c_c, the assembly occurs; below the c_c, the disassembly occurs. Addition and loss of subunits occur at both ends in the case of actin filaments. Addition and loss of subunits occur preferentially at one end, the barbed end (the plus end, see the next paragraph) in the case of microtubules. Both *in vivo* (i.e. in a living cell) and *in vitro* (i.e. in a test tube), subunits of cytoskeletal filaments could form nuclei in a concentration c over the critical concentration c_c. In the growth phase, (II), the nucleated filaments grow until the surrounding concentration become the critical concentration c_c. And in the steady-state phase, (III), the filaments reserve its steady-state length, as the surrounding concentration stays equal to the critical concentration. This steady state is a non equilibrium state with the energy dissipation.

Polarity of cytoskeletal filaments

Actin filaments grow faster at one end than the other end. Microtubules also grow faster at one end than the other end. Faster growing end is called plus end or barbed end and the other end is called minus end or pointed end. So actin filaments and microtubules are polar. The difference of growth between one end and the other is caused by the reason that their subunits are arranged head-to-tail in the protofilaments. But intermediate filaments may not be polar because its coiled-coil subunits are arranged in parallel in the protofilaments.

Treadmilling of cytoskeletal filaments

Cytoskeletal filaments exhibit dynamic phenomena that are pronounced at c_c: treadmilling, the addition of subunits at one end (i.e. a barbed end) and their loss at the other end (i.e. a pointed end). This phenomena has been observed in vivo [18] and in vitro [19] in the case of the actin filaments. And it has been also observed in vivo [20] and in vitro [21] in the case of microtubule.

Dynamic instability of cytoskeletal filaments

A steady-state filament is either growing, shrinking, or undergoing small diffusive fluctuations in length. In contrast, microtubules *in vitro* [1, 22] and *in vivo* [3] are observed to switch between phases of growth and shrinkage. Such behavior has been termed dynamic instability [22]. The switching from shrinkage to growth is called rescue and the switching from growth to shrinkage is called catastrophe. The growth velocity ($\sim 1\ \mu$m/min) is more slowly than the shrinkage velocity ($\sim 10\mu$m/min).

Here I summarize the polymerization of cytoskeletal filaments in Table 1.4.

cytoskeletal filament	microtubule		actin filament		intermediate filament	
	in vitro	*in vivo*	*in vitro*	*in vivo*	*in vitro*	*in vivo*
Polarity	◯	◯	◯	◯	–	–
Treadmilling	◯	◯	◯	◯	–	–
Dynamic instability	◯	◯	–	–	–	–

Table 1.4: Polymerizations of Cytoskeletal Filaments

1.3 Theoretical background of cytoskeletal filaments

1.3.1 The Oosawa's equilibrium and kinetic theories

F. Oosawa was a pioneer of the polymerization of a helical polymer and a polyhedral polymer. Using a simple mathematical model of polymerization similar to that used in polymer chemistry conventionally, he and his co-workers were able to accurately model the assembly of a number of self-assembling proteins. Much of their work concentrated on actin and bacterial flagella, but they also reproduced a variety of other, less easily modeled, self-assembling protein structures.

Equilibrium theory of linear polymerization

I consider the equilibriums describing the addition of a monomer (A_1) onto a i-mer (A_i). Each addition takes place with the same standard-state free energy, given by the dissociation constant K (The equilibrium theory is based on the law of mass action (to see Appendix 3.1)).

$$A_i + A_1 \underset{k_{i+1}^{\mathrm{off}}}{\overset{k_i^{\mathrm{on}}}{\rightleftharpoons}} A_{i+1}, \qquad \frac{c_1 c_i}{c_{i+1}} = K_{i+1} = \frac{k_{i+1}^{\mathrm{off}}}{k_i^{\mathrm{on}}}, \tag{1.1}$$

where c_i stand for the concentration [2] of i-mer, k^{on} and k^{off} are the rate constants of the association and the dissociation, respectively. From the above equation, if K_i is independent of i, the i-mer concentration is related with monomer concentration as below,

$$c_i = K \left(\frac{c_1}{K}\right)^{i-1} \tag{1.2}$$

The total concentration c_{tot} is as below (see Appendix A),

$$\begin{aligned} c_{\mathrm{tot}} &= \sum_{i=1}^{\infty} i c_i \\ &= K \sum_{i=1}^{\infty} i \left(\frac{c_i}{K}\right)^i \\ &= \frac{c_1}{\left(1 - \frac{c_1}{K}\right)^2}. \end{aligned} \tag{1.3}$$

[2] Though the concentration is denoted by $[A_i]$ conventionally, I consistently denote the concentration as c_i through this thesis in order to avoid misunderstanding.

And the average degree of polymerization is defined by,

$$\langle i \rangle = \frac{\sum_{i=1}^{\infty} i c_i}{\sum_{i=1}^{\infty} c_i} \tag{1.4}$$

and becomes to be

$$\langle i \rangle = \frac{1}{1 - \frac{c_1}{K}}. \tag{1.5}$$

This doesn't say the behavior of the polymerization such as cytoskeletal filaments. This behavior is that the average degree of polymerization increases slowly as the total concentration increases.

Equilibrium theory of helical polymerization

Oosawa's idea is that the polymer adds a small number of monomers (I denote this n.) in the usual linear scheme (with linear dissociation constant K), but then the polymer curls around on itself to start a helix. Once the first turn has been made (where he introduce a critical size [3] which make a turn), the subsequent additions of monomer are much more favorable because they interact with the monomer bellow them. I denote this more favorable dissociation constant of monomer subtractions beyond the first turn as $K_{\rm h}$ and assume that $K_{\rm h} > K$ (Typically, $K_{\rm h}/K \sim 10$ or 100). Then the i-mer concentration is as below (as same as the above paragraph),

$$c_i = \sigma K_{\rm h} K \left(\frac{c_1}{K_{\rm h}} \right)^{i-1}, \tag{1.6}$$

where $\sigma = (K/K_{\rm h})^{i-1} \ll 1$. And the total concentration is derived as below (refer to Appendix A),

$$\begin{aligned} c_{\rm tot} &= \sum_{i=1}^{\infty} i c_i \\ &= \sum_{i=1}^{n} i c_i + \sum_{i=n+1}^{\infty} i c_i \\ &= c_1 + K \sum_{i=2}^{n} i \left(\frac{c_i}{K} \right)^i + \sigma K \sum_{i=n+1}^{\infty} i \left(\frac{c_i}{K_{\rm h}} \right)^i \end{aligned}$$

[3] This critical size is an analogy of that in the classical nucleation theory [23].

$$
\begin{aligned}
&= c_1 + K\sum_{i=2}^{n} i\left(\frac{c_i}{K}\right)^i + \sigma K\sum_{i=1}^{\infty} i\left(\frac{c_i}{K_\mathrm{h}}\right)^i - \sigma K\sum_{i=1}^{n} i\left(\frac{c_i}{K_\mathrm{h}}\right)^i \\
&= c_1 + \frac{\sigma c_1}{\left(1-\frac{c_1}{K_\mathrm{h}}\right)^2} + \left(\sigma c_1 + 2\sigma\frac{c_1^2}{K_\mathrm{h}}\right) \qquad (1.7)
\end{aligned}
$$

This says that as c_1 is increased from zero, first, all the monomers stays as monomer. But at a certain critical concentration c_c, suddenly all additional monomer goes into helical polymer, and the concentration of monomer stays essentially constant i.e. c_c. And the average degree of polymerization of helical polymer is as below,

$$
\begin{aligned}
\langle i\rangle &= \frac{\sum_{i=n}^{\infty} ic_i}{\sum_{i=n}^{\infty} c_i} \qquad (1.8) \\
&= \frac{1}{1-\frac{c_1}{K_\mathrm{h}}} \qquad (1.9)
\end{aligned}
$$

The behavior of this resembles the polymerization of cytoskeletal filaments so much. The average length $\langle i\rangle$ becomes so large as the total concentration goes over the critical concentration. And the result resemble the gas-liquid transition expressed by the van der Waals equation of state [24]. Dispersed monomers (and linear polymers) correspond to gas molecules and helical polymers correspond to liquid.

Kinetic theory of linear and helical polymerization

The Oosawa's kinetic theory, in essence, treats the growth rate of a polymer as being independent of its length, once the polymer is larger than a certain critical size, known as the stable nucleus size. For a polymer larger than this size, the growth of the polymer can be expressed as a combination of a growth rate, multiplied by the concentration of available free monomers that can be bound, minus the dissociation rate (or off rate) of bound monomers breaking away from the polymer.

For a given polymer of sufficient size, the growth rate v is

$$v = k^{\mathrm{on}}c_1 - k^{\mathrm{off}}, \qquad (1.10)$$

where k^{on} stands for the binding rate of free monomers to the polymer, k^{off} stands for

the loss rate of bound monomers from the polymer, c_1 stands for the concentration of free monomers to be bound.

Applied to a single polymer, the above equation must be interpreted in terms of probabilities, since the binding and loss rates are only accurate in aggregate. However, this equation can be used to provide a description of the change in the population of all polymers with subunits of size i, and hence a description of the population of all polymers;

$$\frac{dc_i}{dt} = +k_{i+1}^{\text{off}} c_{i+1} - k_i^{\text{on}} c_i c_1 + k_{i-1}^{\text{on}} c_{i-1} c_1 - k_i^{\text{off}} c_i, \tag{1.11}$$

where c_i stands for the concentration of polymers of size i subunits, t stands for time, k^{on} stands for the binding rate of free monomers to the polymer, k^{on} stands for the loss rate of bound monomers from the polymer c_1 stands for the concentration of free monomers to be bound. This equation tells that the number of polymers of a particular size i subunits increases as polymers of size $i+1$ shrink to size i (the first term), decreases as polymers of size i grow to a larger size (the second term), increases as smaller polymers of size $i-1$ grow to size i (the third term) and decreases as polymers of size i lose monomers and sink to size $i-1$ (the last term). Since the rate constants are assumed under this model to be independent of polymer size, they are constant for all size $i > i_0$, where i_0 stands for a critical size of a nucleus.

A similar equation is used to describe the production of nuclei, that is polymers of critical size, that are assumed to have different on and off rates:

$$\frac{dc_{i_0}}{dt} = +k_{i+1}^{\text{off}} c_{i_0+1} - k_i^{\text{on}} c_{i_0} c_1 + k_{i-1}^{\text{on}^*} c_1^{i_0} - k_i^{\text{off}^*} c_{i_0}, \tag{1.12}$$

where, in addition to the variables described above, k^{on^*} is the creation rate of nuclei from free monomers, k^{off^*} is the destruction rate of nuclei to free monomers.

By fitting these two equations with experimentally observed data, they conclude that the polymerization in the case of actin filament is a helical polymerization with $i_0 = 3.5$. For some other proteins the Oosawa's kinetic theory produces accurate results.

1.3.2 Kinetic model for the treadmilling

A. Wegner observed the exchange of subunits at the ends of actin filaments using the radioactively labeled actin monomers and found a polymerization mechanism in which the filaments grow at one end and shrink simultaneously at the other end (head to tail polymerization) [19].

Critical concentration for bidirectional polymerization

Consider the simple case of bidirectional growth from a polar polymer not involving nucleotide hydrolysis. We can write the rates at the barbed and pointed ends as:

$$\frac{dn_B}{dt} = k_B^{\text{on}} c - k_B^{\text{off}} \tag{1.13}$$

and

$$\frac{dn_P}{dt} = k_P^{\text{on}} c - k_P^{\text{off}}, \tag{1.14}$$

where dn_B/dt and dn_P/dt are the net rates of elongation in units of number of subunits, n, added per second per polymer at the barbed and pointed ends respectively; k_B^{on} and k_B^{on} are respective association rate constants, k_B^{off} and k_B^{off} are respective association rate constants, c stands for the monomer concentration. In the steady state,

$$\frac{k_B^{\text{off}}}{k_B^{\text{on}}} = \frac{k_P^{\text{off}}}{k_P^{\text{on}}} = K, \tag{1.15}$$

where K stands for the dissociation constant, both ends has the same critical concentration, c_c (here $c_c = K$) [4].

Critical concentration for the treadmilling

In the treadmilling scheme of Wegner, assembly is coupled to nucleotide triphosphate hydrolysis to allow pathways of monomer addition and removal in which certain steps can be made to proceed at a negligible rate. I call a monomer binding triphosphate and a monomer binding diphosphate T and D monomers, respectively. There are four major pathways: T monomers attachings at both ends (I denote the rate constants of association at barbed end and pointed end as k_{BT}^{on} and k_{PT}^{on}, respectively) and D

[4] For this simple relation of the polymerization, I adopt the dissociation constant as for the equilibrium constant in this thesis instead of the association constant though I do not state heretofore.

filamentous monomers dettachings at both ends (I denote these rate constants as k_{BD}^{off} and k_{PD}^{off}). The net rates at each end are given by:

$$\frac{dn_B}{dt} = k_{BT}^{\text{on}} c - k_{BD}^{\text{off}} \tag{1.16}$$

and

$$\frac{dn_P}{dt} = k_{PT}^{\text{on}} c - k_{PD}^{\text{off}}, \tag{1.17}$$

Although the equations are the asame form as those given above for bidirectional polymerization, eqs 1.13 and 1.14, the pairs of rate constants k_{BT}^{on}, k_{PT}^{on} and k_{BD}^{off}, k_{PD}^{off} are no longer the association and dissociation rates of the same reactions. Therefore $k_{BD}^{\text{off}}/k_{BT}^{\text{on}}$ need not in general be equal to $k_{PD}^{\text{off}}/k_{PT}^{\text{on}}$. The overall growth rate is the sum of eqs 1.16 and 1.17, and it defines a critical concentration. This critical concentration is given by Wegner [19]:

$$c_c = \frac{k_{BD}^{\text{off}} + k_{PD}^{\text{off}}}{k_{BT}^{\text{on}} + k_{PT}^{\text{on}}} \tag{1.18}$$

This scheme allows the critical concentration to be different for each end. The critical concentrations for the barbed and pointed ends are given by:

$$c_{c_B} = \frac{k_{BD}^{\text{off}}}{k_{BT}^{\text{on}}} \tag{1.19}$$

and

$$c_{c_P} = \frac{k_{PD}^{\text{off}}}{k_{PT}^{\text{on}}}. \tag{1.20}$$

1.3.3 Reaction-diffusion model for the dynamic instability

M. Dogterom and S. Leibler analyzed the dynamic instability using a stochastic model expressed by the following reaction-diffusion equations [25]:

$$\frac{\partial p_+(i,t)}{\partial t} = -v_+ \frac{\partial p_+(i,t)}{\partial i} - f_{+-} p_+(i,t) + f_{-+} p_-(i,t), \tag{1.21}$$

$$\frac{\partial p_-(i,t)}{\partial t} = v_- \frac{\partial p_-(i,t)}{\partial i} + f_{+-} p_+(i,t) - f_{-+} p_-(i,t), \tag{1.22}$$

where $p_+(i,t)$, $p_+(i,t)$ stand for the probability that a polymer is growing or shrinking i-mers, respectively, v_+,v_- stand for the growth and shrinkage rates, respectively, f_{+-},f_{-+} stand for the catastrophe and rescue rates, respectively. The model predicts a sharp conversion between bounded growth and unbounded growth pending

on whether $f_{+-}v_- - f_{-+}v_+$ is greater than or less than zero. Under conditions that lead to bounded growth, the length of the microtubules are distributed exponentially with mean length:

$$\langle i \rangle \cong \frac{v_- v_+}{v_- f_{+-} - v_+ f_{-+}} \tag{1.23}$$

This equation has a simple interpretation: ignoring rescue (i.e., setting $f_{-+} = 0$), it says that the mean length equals the growth rate (v_+) times the average duration of the growth phase ($1/f_{+-}$).

1.4 Purpose of the thesis

On the basis of the above background, one of the purpose of this thesis is to construct a self-continued stochastic models for the dynamics of cytoskeletal filaments; the model should have some intrinsic connections with the macroscopic as well as the microscopic models. In particular, the model should reproduce, in statistical average, the result of Oosawa's theory. On the other hand, the model should reflect suitable symmetry and conservation laws of microscopic physics. Furthermore I expect that the model should perform the microtubule's dynamical phenomena such as the dynamic instability.

And another purpose is to reveal the characteristic properties of the growth-shrinkage dynamics by using the constructed two-dimensional mesoscopic model, to analyze the growth-shrinkage dynamics and to clarify the relations between the concentration and the velocity of the growth and shrinkage phases.

1.5 Structure of the thesis

In this thesis, I introduce a lattice polymerization model for the dynamics of cytoskeletal filaments in Chapter II and introduce an kinetic model of linear polymerization with a threshold length in a finite volume system in Chapter III. And I show the results of the lattice model without internal state dynamics and the results of the kinetic model in Chapter IV. Also I show the results of the lattice model with internal model in Chapter V. Finally, I summarize this thesis in Chapter VI.

Chapter 2

A lattice polymerization model

In this chapter, I introduce a lattice toy model which simulates the dynamics of the cytoskeletal filaments, which I and K. Ebina proposed in [26, 27]. I am particularly interested in the polymerization of tubulin dimers into microtubules and their behavior called dynamic instability. The goal is to construct a self-contained mesoscopic model of the dynamics of cytoskeletal filaments; the model should have some intrinsic connections with the macroscopic as well as the microscopic models. In particular, the model should reproduce, in statistical average, the result of Oosawa's theory[7], where a thermodynamic and kinetic discussion of linear assemblies are given. On the other hand, the model should reflect suitable symmetry and conservation laws of microscopic physics. Furthermore I expect that the model should perform the dynamical phenomena of cytoskeletal filaments such as the dynamic instability.

2.1 Essential physical ingredients for the dynamics of cytoskeletal filaments

Though there are some kinetic explanations to the phenomenon of dynamic instability (such as the cap model [22] etc.), it is important to construct a quantitative model of the cytoskeletal filaments taking account of the spatial effects, having an ability to show dynamic instability. In order to construct a reasonable toy model for the dynamic instability, I assume that the next three physical ingredients play essential roles in these phenomena: (a) random motion of subunits in space, (b) short range and electrostatic interaction between subunits with a threshold length, and (c) in-

ternal state dynamics of each subunit [1], though other fluid dynamical effects such as the convection and/or electromagnetic interaction effects might play some important roles. I extract the ingredient (a) because the molecular weight of a cytoskeletal subunit is around 10^5 much larger than atoms and much smaller then visible particles so that a subunit takes a Brownian motion by the thermal fluctuation in an electrolyte (cytoplasm or simply water) if existing freely. This shows a diffusion phenomena macroscopically. I extract the ingredient (b) because it is important to take of structural changes such as the change from a linear structure to a helical structure for proper understanding of the growth of helical object, according to Oosawa's theory [7]. And I extract the ingredient (c) because a subunit takes two state: GDP-binding state and GTP-binding state in the case of a tubulin, ATP-binding state and ADP-binding state in the case of a actin and non-hydrolyzed state and hydrolyzed state in the case of a intermediate filament. I mainly focus my attention to phenomena of the time scales of seconds or minutes; it is practical to adopt a lattice model (not a continuous model) for simulations. I ignore the detailed geometrical (helical) structure of a cytoskeletal filament: I make up a linear (one dimensional) growth/shrinkage model in two dimensions simply.

2.2 A lattice polymerization model for the dynamics of cytoskeletal filaments

In the two-dimensional lattice model, I treat cytoskeletal subunit as a particle. A particle occupy one lattice site. For the random motion in space, (a), I use a random walk model. The excluding volume effects are taken into account (i.e. an extended lattice gas model[29]). The concentration c in the two-dimensional lattice system is defined as $c = N/XY$, where N is the total number of particles, X and Y are, the horizontal and vertical linear dimensions of the system, respectively. The time scale for one step of polymerizations τ_a is related with the concentration as $\tau_a \sim c^{-2/d}$ (d = 2 for two dimensions) for dilute systems.

[1] In the articles[26, 27, 28], I treat random motion of subunits in space, (a), as (a') diffusion; I treat short range and electrostatic interaction with a threshold length, (b), dividing to (b')short range and electrostatic interaction and (c') structural change; and I treat internal state dynamics, (c), as (d') chemical reaction.

By short range interaction, (b), two particles in the nearest neighbor sites in the specific direction become lower energy state and tend to polymerize. Because of the electrostatic dipole interaction two molecules tend to align. At the present stage, I simply ignore the detailed form of the long-range part of the electrostatic interaction because of the Debye shielding of ionic cytoplasm. I assume that particles which occupy sites side-by-side relation to each other in the specific (horizontal) direction belong to the same polymer. Then I define a length of polymer as the number of particles which belong to the same polymer. Though the nucleation process has not been understood, the linear structure of polymerized subunits could tend to become a helical structure. To mimic this effect, I introduce a threshold length $l_{\rm th}$: a particle belonging to and being at the edge of a linear polymer will easily detach if the length l of the linear polymer is shorter than the threshold $l_{\rm th}$ (*i.e.* $< l_{\rm th}$), while it tends to stick more tightly if $l > l_{\rm th}$. So I assume that a length of a cytoskeletal filament, l, exceed some threshold value $l_{\rm th}$, the helical structure should be more stabilized.

I treat the internal dynamics in each subunit, (c), as one inner degree of freedom of two states: GDP-binding state and GTP-binding state in the case of a tubulin, ATP-binding state and ADP-binding state in the case of a actin and non-hydrolyzed state and hydrolyzed state in the case of a intermediate filament. Though some structural change would take place in a subunit, we could consider that this inner degree of freedom corresponds to a chemical reaction coordinate λ. I take the discrete coordinate for simplicity. In this model I assume that the state of a tubulin is GTP if $\lambda \geq 0$ and that the state of a tubulin is GDP if $\lambda < 0$ and I assume that those in the cases of an actin and an IF protein. I then call the state of a particle with GTP(ATP) the **T** state, GDP(ADP) the **D** state, respectively though in the case of IF protein the non-hydrolyzed and hydrolyzed states correspond to these. The value of this coordinate decreases deterministically by one in one step for particles in a polymer of $l \geq l_{\rm th}$ (I call them P particles where P is named after polymer) and increases deterministically by one in one step for particles in a polymer of $l < l_{\rm th}$, including isolated ones (I call them M particles where M is named after monomer). I restrict that the value of the coordinate has an upper bound $\tau_D (> 0)$ and lower bound $\tau_T (< 0)$. These upper and lower bounds are parameters which determines the

attach-detach time scales.

As for the effect of the short range interaction, I incorporate all the effect in the probability of a particle transfer to unoccupied sites, the environment of the considered particle is shown in Table4.44. The parameters p^C_{AB} in Table4.44 determines the probability of depolymerizations. Sub- and super- scripts A, B, C stands for the ends, the internal states and the P or M states, respectively.

Occupation of Sides	$\mathrm{M}_{\mathbf{T}}$	$\mathrm{M}_{\mathbf{D}}$	$\mathrm{P}_{\mathbf{T}}$	$\mathrm{P}_{\mathbf{D}}$
$\cdot\bullet\cdot$	$\frac{1}{4}$	$\frac{1}{4}$	$\frac{1}{4}$	$\frac{1}{4}$
$\circ\bullet\cdot$	p^M_{BT}	p^M_{BD}	p^P_{BT}	p^P_{BD}
$\cdot\bullet\circ$	p^M_{PT}	p^M_{PD}	p^P_{PT}	p^P_{PD}
$\circ\bullet\circ$	0	0	0	0

Table 2.1: The probability of a particle transfer depending on various situations. T and D stand for the inner state of a particle in the time, The considered particle is denoted as $\bullet$, while "empty" site is denoted as $\cdot$ and "occupied" site as $\circ$.

2.3 Measurement of length

I measure the lengths of polymers by the polymer labeling method which I modify the cluster multiple method of J. Hoshen and R. Kopelman [30] for the lattice polymerization model. I assign polymer labels to sites beginning at the upper left corner in the two dimensional lattice and continue from left to right checking the occupancy of each site along each row. If a site is occupied, I check the occupancy of its left nearest neighbor. If the left neighbor is unoccupied, I assign the next available polymer label. If the left neighbor is occupied, the site is assigned the label of its occupied neighbor. And I use the periodic boundary condition.

Chapter 3

An effective kinetic model

In this section, I introduce an effective kinetic model for linear polymerization of cytoskeletal filaments with a threshold length in a finite volume system in order to show the importance of the threshold length in the nucleation phase and understand the kinetic constant accurately and to understand the shifted peak shown in the lattice polymerization model (to see the section 4.2). I analyze this model numerically. Finally, I discuss the relationship between this model and the real biological system.

3.1 Polymerization

Polymerization processes for cytoskeletal filaments could be classified to three phases: (I) a nucleation phase (also called lag phase), (II) a growth phase (also called polymerization phase) and (III) a steady-state phase (also called equilibrium phase). In (I) the nucleation phase, subunits create a stable nucleus by the thermal fluctuation in the concentration c which is larger than a critical concentration c_c. The time of this nucleation phase is a few minutes. The mechanism of the nucleation has not been resolved yet. But the existence of a threshold length is important for the nucleation in the linear polymerization as same as the critical size is important in the case of droplets on the classical nucleation theory [23].

In (II) the growth phase, monomers polymerizes to a filament so that the monomer concentration continues to decrease to the balancing concentration (so called critical concentration). In the experiments, the growth velocity, v, is measured in this growth phase. From the result of v in several initial concentration, c_0, the kinetic constants of

on-reaction, $k^{\rm on}$, and off-reaction, $k^{\rm off}$, are derived on the basis of the linear equation as below,

$$v = k^{\rm on} c_0 - k^{\rm off} \tag{3.1}$$

Sometimes this equation causes a misunderstanding: c_0 is the initial concentration and the concentration after the nucleation is not equal to c_0. This equation is very simple. So the kinetic constants are determined by this equation conventionally.

In (III) the steady-state phase, the monomer concentration and the polymer concentration keep constant values approximately. The monomer concentration in this phase is thought to be the critical concentration. Even if these concentrations have little change, we need to recognize that this is the non equilibrium state with the energy flow (in the case of actin filament, the hydrolysis of ATP on the subunits in filament and the nucleotide exchange on the monomer subunits).

3.2 An Effective Kinetic Model

I consider that subunit monomers polymerize linearly. I denote the polymers of length l as $A_l (l = 1, 2, ..., L)$ where L is the maximum length of polymers and consider the reaction kinetics of polymers as follow,

$$A_l + A_1 \underset{k^{\rm off}_{l+1}}{\overset{k^{\rm on}_l}{\rightleftharpoons}} A_{l+1}, \tag{3.2}$$

where $k^{\rm on}_l$ and $k^{\rm off}_{l+1}$ stand for the rate constant of a linear polymer from length l to $l+1$ and from $l+1$ to l, respectively. I treat a monomer concentration c_1 explicitly in order to understand the polymerization with the conservation of total concentration. I denote the concentration of polymers with length l as c_l. The kinetic equation of the concentration of polymers with length l is expressed as follows,

$$\frac{dc_l}{dt} = +k^{\rm off}_{l+1} c_{l+1} - k^{\rm on}_l c_l c_1 + k^{\rm on}_{l-1} c_{l-1} c_1 - k^{\rm off}_l c_l. \tag{3.3}$$

Monomers polymerize to and depolymerize from aggregates of all length i.e. $2 \leq l \leq L$. So the kinetic equation of the concentration of monomers c_1 is expressed as follows,

$$\frac{dc_1}{dt} = -\sum_{l=1}^{L-1} k^{\rm on}_l c_l c_1 + \sum_{l=2}^{L} k^{\rm off}_l c_l. \tag{3.4}$$

The conservation of the total number of subunits is derived from above equations 3.3 and 3.4 by treating the boundary condition appropriately.

$$\begin{aligned}\frac{d}{dt}\sum_{l=1}^{L} l c_l &= +\sum_{l=1}^{L-1} l k_{l+1}^{\mathrm{off}} c_{l+1} - \sum_{l=1}^{L-1} l k_l^{\mathrm{on}} c_l c_1 + \sum_{l=2}^{L} l k_{l-1}^{\mathrm{on}} c_1 - \sum_{l=2}^{L} l k_l^{\mathrm{off}} c_l \\ &\quad +1\sum_{l=2}^{L} k_l^{\mathrm{off}} c_l - 1\sum_{l=1}^{L-1} k_l^{\mathrm{on}} c_l c_1 \\ &= 0. \end{aligned} \tag{3.5}$$

Next I introduce a threshold length l_{th}. Helical or tubular filament such as microtubule or actin filament has a critical concentration of polymerization [10]. So I treat polymers with length $l(\geq l_{\mathrm{th}})$ is more stable than polymers of length $l(< l_{\mathrm{th}})$ energetically. I define the kinetic constant $(k_l^{\mathrm{on}}, k_l^{\mathrm{off}})$ depending on length as follows,

$$k_l^{\mathrm{on}} = \begin{cases} k_m^{\mathrm{on}} & 1 \leq l < l_{\mathrm{th}} \\ k_p^{\mathrm{on}} & l_{\mathrm{th}} \leq l < L \\ 0 & l = L \end{cases} \tag{3.6}$$

$$k_l^{\mathrm{off}} = \begin{cases} 0 & l = 1 \\ k_m^{\mathrm{off}} & 1 < l < l_{\mathrm{th}} \\ k_p^{\mathrm{off}} & l_{\mathrm{th}} \leq l \leq L, \end{cases} , \tag{3.7}$$

where $k_m^{\mathrm{on}}, k_p^{\mathrm{on}}, k_m^{\mathrm{off}}, k_p^{\mathrm{off}}$ are the positive values corresponding to the rate constants for linear polymer (the subscripts p and m is named after monomer and polymer.) and k_m^{off} is larger than k_p^{off} because of the energetics and I assume $k_m^{\mathrm{on}} = k_p^{\mathrm{on}}$ for simplicity.

Chapter 4

Results I: models with threshold length

In this chapter I show the results in the lattice polymerization model without the internal state dynamics and I also show the results in the effective kinetic model for linear polymerization. First of all, I show the results in two limiting cases of the lattice polymerization model in low concentration. Next I show the results in the several possible cases of the lattice polymerization model. Then I show the characteristic result of length distribution of polymers in the specific case of the lattice polymerization model with the detach probability. Finally I show the some results in the effective kinetic model in order to understand the above characteristic distribution.

4.1 Results in the lattice polymerization model without the internal state dynamics

In the most general form, the lattice polymerization model contains three physical ingredients (a) – (c) described in chapter 2. Then I have to assign several parameters such as the detach probability to the nearest neighbor sites for each particle, the rate of the chemical reaction and the polymerization threshold length.

Here I simplify the lattice polymerization model by neglecting the internal state dynamics of subunits ($T \leftrightarrow D$) and the polarity (B or P) [28]. Therefore the set of parameters reduces to be as shown in Table 4.1 , where I assume that the detach probability of monomer p^M is 1/4 naturally and describe the detach probability of

polymer subunit p^P as $p_{\rm d}$.

Occupation of Sides	M	P
$\cdot \bullet \cdot$	1/4	1/4
$\circ \bullet \cdot$ or $\cdot \bullet \circ$	1/4	$p_{\rm d}$
$\circ \bullet \circ$	0	0

Table 4.1: The parameter $p_{\rm d}$ stands for the detach probability of a particle transfer depending on various situations and can have a value of $0 \leq p_{\rm d} \leq 1/4$. M and P stand for the states of a particle: monomer and polymer respectively in the time. The considered particle is denoted as $\bullet$, while "empty" site is denoted as $\cdot$ and "occupied" site as $\circ$.

4.1.1 Two limiting cases: DLA and LGM in low concentrations

The parameter $p_{\rm d}(0 \leq p_{\rm d} \leq 1/4)$ in Table 4.1 stands for the detach probability of a polymer subunit to the nearest neighbor sites. The limiting case $p_{\rm d} = 0$ corresponds to the DLA [31], while the other limiting case $p_{\rm d} = 1/4$ corresponds to the LGM with a constraint of the vertical motion. In simulations I use a system of N particles in the two dimensional lattice with width Y and length X so that the total concentration c becomes N/XY. I use the periodic boundary condition.

I perform simulations in the above two limiting cases (DLA & LGM) in the region of low concentrations $c \leq 0.05$ with the initial condition of a prepared polymer of length l=100 in the lattice of $X = 300$ and $Y = 100$.

The time series of the length l of a polymer in DLA in low concentrations c are shown in Fig.4.1 and the values of the growth velocity $v_{\rm g} \equiv dl/dt$ of a polymer and its averages are shown in Fig.4.2. In Fig.4.1 we see that the length increases as the concentration increases. From Fig.4.2 I conclude that the growth velocity of a polymer increases linearly with the concentration. The line which connects the averaged growth velocity $\bar{v_{\rm g}}$ at each concentration is expressed by $\bar{v_{\rm g}} = a(c - c_0)$, where $c - c_0$ plays a role as effective concentration with $c_0 \simeq 0.0033$ and the coefficient a is estimated to be 0.45 with standard deviation of 0.02. The reason why the point of

intersection of the above line and the concentration axis is shifted from the origin is partly because of the particles consisting a polymer is also counted in the definition of concentration.

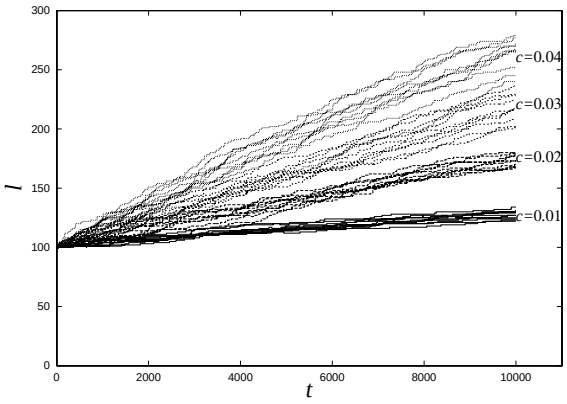

Figure 4.1: The time series of the length l of a DLA single polymer for 10,000 steps period in several low concentrations: t stand for the steps per particle in the system and c stands for the concentration of a system.

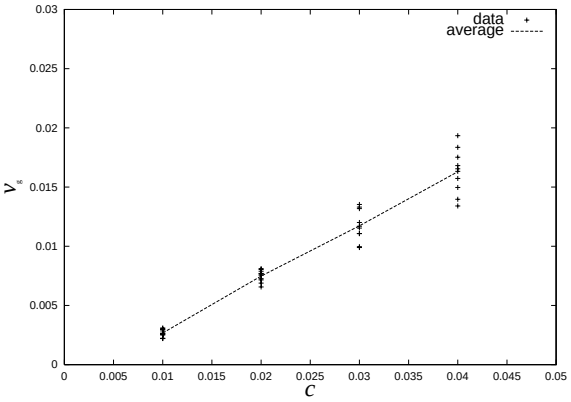

Figure 4.2: The growth velocity $v_{\rm g}$ of a DLA single polymer and its average as a function of the concentration c. The average growth velocity is connected with the dotted line: $\bar{v_{\rm g}} = 0.45(c - 0.0033)$

The time series of the length in LGM in low concentrations c are shown in Fig.4.3 and the values of the shrinkage velocity $v_{\rm s} \equiv dl/dt$ of a polymer and its averages are shown in Fig.4.4. In Fig.4.3 I see that the length decreases similarly in all the concentrations. From Fig.4.4 I conclude that the shrinkage velocity $\bar{v_{\rm s}}$ of a polymer is almost constant; i.e. mainly dependent of the detach probability. The line which connects the averaged shrinkage velocity $\bar{v_{\rm s}}$ at each concentration is expressed by $\bar{v_{\rm s}} = -0.97 \pm 0.10$.

Summary and discussions

I perform simulations of the lattice polymerization model in two limiting cases of a diffusion-limited aggregation model and a simple lattice gas model. These cases show important features in the cytoskeletons' dynamics: in low concentrations, the growth velocity of a polymer increases linearly as the concentration increases, while the shrinkage velocity of a polymer mainly depends on the detach probability. These

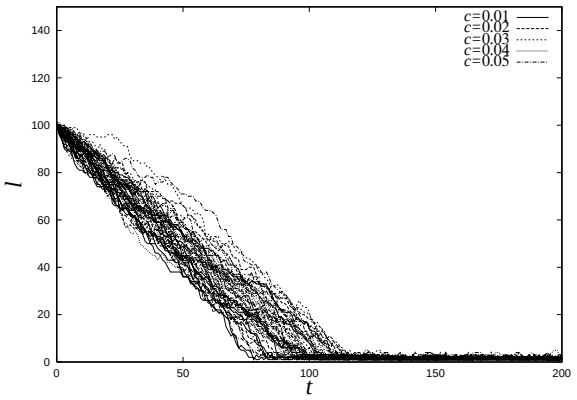

Figure 4.3: The time series of the length l of a LGM single polymer for 200 steps period in several low concentrations: t stand for the steps per particle in the system and c stands for the concentration of a system.

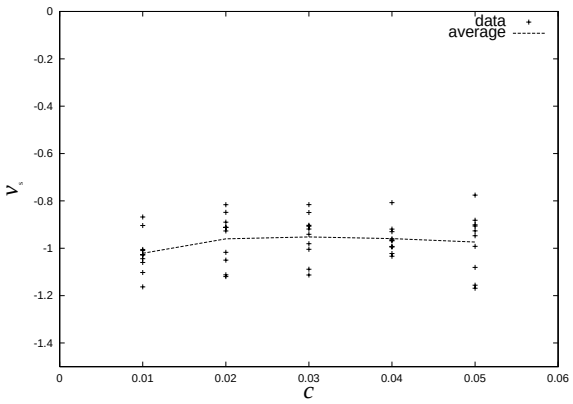

Figure 4.4: The shrinkage velocity $v_{\rm s}$ of LGM single polymer and its average vs. concentration c. The average shrinkage velocity is connected with the dotted line: $\bar{v_{\rm s}} = -0.97 \pm 0.10$

results will be important for the understanding of the growth-shrinkage dynamics of cytoskeletal filaments such as dynamic instability.

In DLA, the both ends of a polymer may be considered to be sinks of subunits. The problem of diffusion with a sink is described by the Laplace equation in the stationary state [32]. A basic solution in two dimensions is expressed by $c(r) = a \log(r/r_0)$, where c is concentration, r is distance from the sink and a and r_0 are constants. The six nearest neighbor sites have a effective concentration $c_{\rm eff}$ then the growth velocity should be $\bar{v_{\rm g}} = (6/4)c_{\rm eff}$. I estimate by using the simulation result of $\bar{v_{\rm g}} = 0.45c$ that the concentration reaches the uniform value at the distance of about $r \sim 3$ sites. This estimation is based on the idea that the both ends of polymer grow up slowly by the diffusion with the logarithmic distribution of concentration around the ends.

In the simulations of LGM, I found that the shrinkage velocity is determined essentially by the detach probability. The both ends of polymer are the source of subunits in contrast to DLA. Applying a similar argument as above with sinks replaced by sources, I estimate that at the distance of about $r \sim 3$ sites the concentration reaches the uniform value, though in this case the process may not be stationary due to the large shrinkage velocity of $\bar{v_{\rm s}} \simeq -1$.

4.1.2 Several cases: possible concentrations and detach probabilities

In the lattice polymerization model without the internal state dynamics, the detach probability could take values between 0 and 0.25 and the concentration also could take values between 0 and 1. So I simulate the lattice polymerization model without the internal state dynamics with several detach probability $p_{\rm d}$ ($0 \sim 0.25$) in the concentration c ($0.1 \sim 0.9$) in two dimensional lattice of $X = 500$ and $Y = 250$ with the threshold length $l_{\rm th} = 10$.

I show the results of time series of length of a prepared polymer for 10,000 steps period in the several cases in Figs.4.5–4.40. We could see many features in these figures.

In the DLA case i.e. $p_{\rm d} = 0$ $c = 0.1 \sim 0.6$ (shown in Figs.4.5–4.10), figures show clear growth phases with each growth velocity and all the values of lengths reach the maximum value of 500. These mean that all the prepared polymers reach the lattice size ($X = 500$). And growth velocity becomes larger as the concentration becomes larger. These correspond to some large concentration regions in the cases of the previous section (DLA).

In the case with $p_{\rm d} = 0.05$ $c = 0.1 \sim 0.6$ (shown in Figs.4.11–4.16), we cloud see both growth and shrinkage phases in different concentrations. In Fig.4.12, the growth/shrinkage phases are almost balancing each other for long steps period (>10,000) so that prepared polymers keeps steady-state length in this case. Also in Fig.4.16, some value of length reach the maximum i.e. 500 and the other value of length couldn't reach the maximum, where the maximum is based on the system size ($X = 500$). These things indicate that many other polymers nucleate and they decrease the free monomer concentration. This is some relationship with the situation that the concentration i.e. $c = 0.6$ is larger than the critical concentration in percolation i.e. $c_c = 0.5$.

In the case with $p_{\rm d} = 0.10$ $c = 0.1 \sim 0.6$ (shown in Figs.4.17–4.22), the values of length decrease in the concentration c (≤ 0.3) and the values of length increase in the concentration c (≥ 0.4). And in the case of large concentration (shown in Fig.4.22), some values of length reach the maximum and the other increase initially

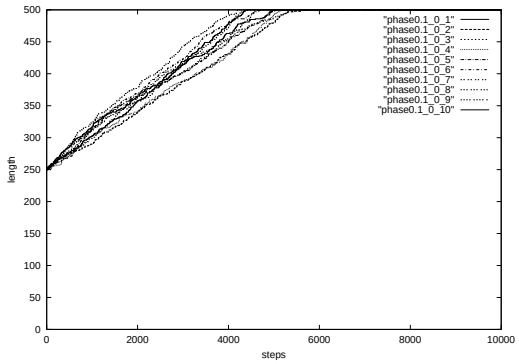

Figure 4.5: Time series of length of a prepared polymer for 10,000 steps period in the case: $c = 0.1, p_{\mathrm{d}} = 0$

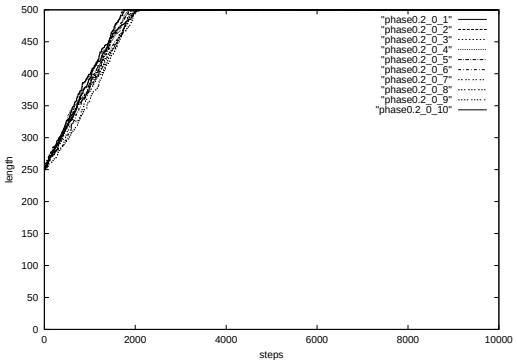

Figure 4.6: Time series of length of a prepared polymer for 10,000 steps period in the case: $c = 0.2, p_{\mathrm{d}} = 0$

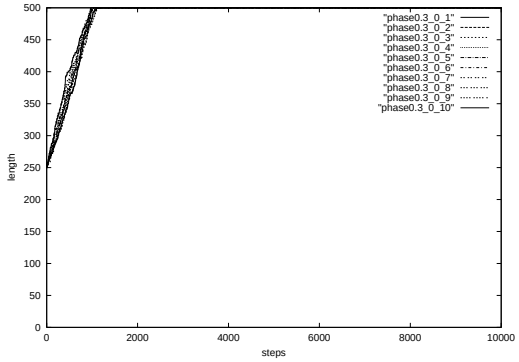

Figure 4.7: Time series of length of a prepared polymer for 10,000 steps period in the case: $c = 0.3, p_{\mathrm{d}} = 0$

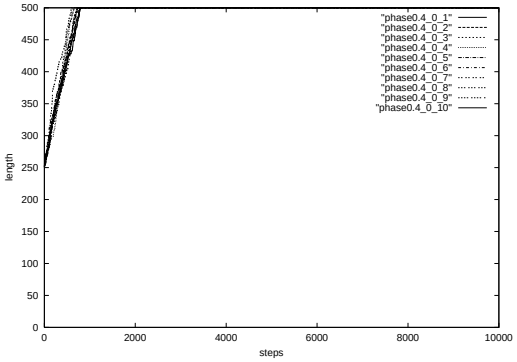

Figure 4.8: Time series of length of a prepared polymer for 10,000 steps period in the case: $c = 0.4, p_{\mathrm{d}} = 0$

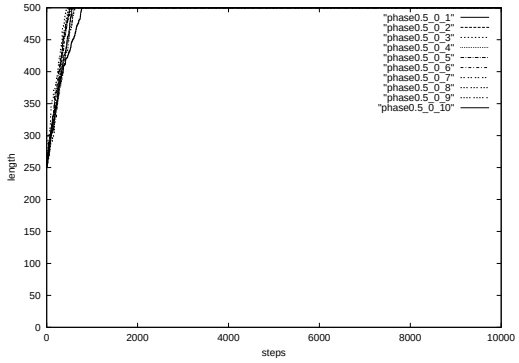

Figure 4.9: Time series of length of a prepared polymer for 10,000 steps period in the case: $c = 0.5, p_{\mathrm{d}} = 0$

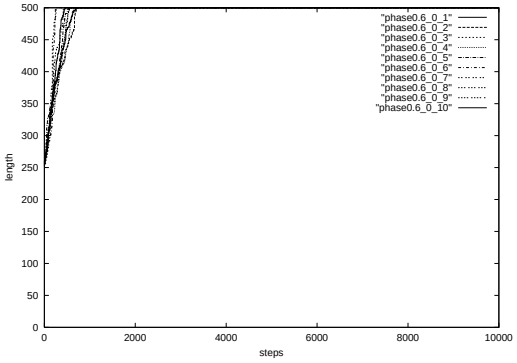

Figure 4.10: Time series of length of a prepared polymer for 10,000 steps period in the case: $c = 0.6, p_{\mathrm{d}} = 0$

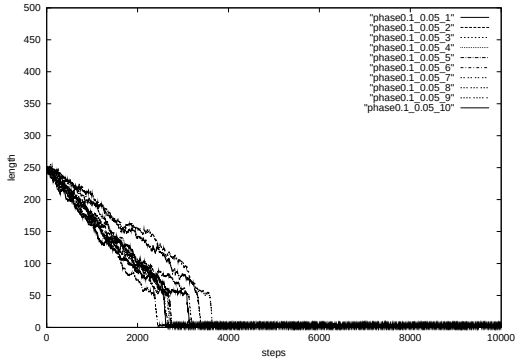

Figure 4.11: Time series of length of a prepared polymer for 10,000 steps period in the case: $c = 0.1, p_{\mathrm{d}} = 0.05$

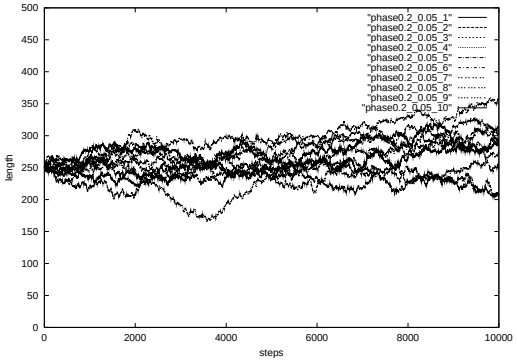

Figure 4.12: Time series of length of a prepared polymer for 10,000 steps period in the case: $c = 0.2, p_{\mathrm{d}} = 0.05$

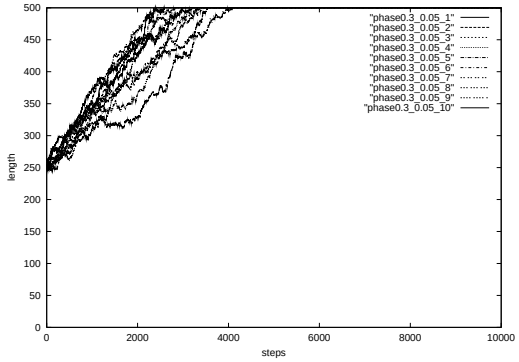

Figure 4.13: Time series of length of a prepared polymer for 10,000 steps period in the case: $c = 0.3, p_{\mathrm{d}} = 0.05$

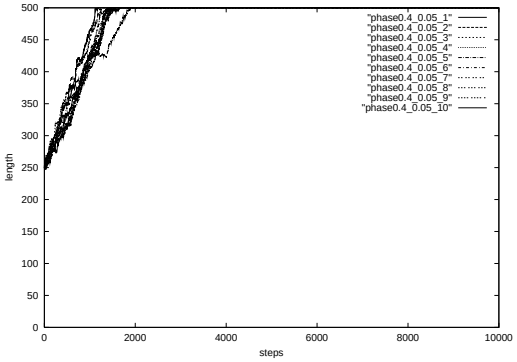

Figure 4.14: Time series of length of a prepared polymer for 10,000 steps period in the case: $c = 0.4, p_{\mathrm{d}} = 0.05$

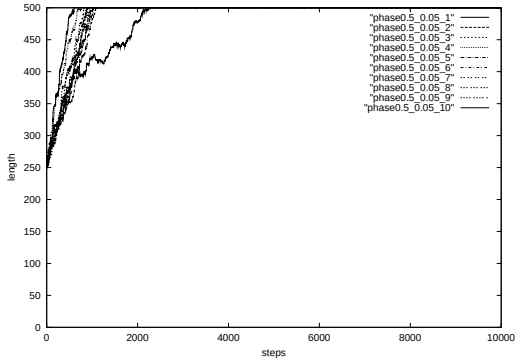

Figure 4.15: Time series of length of a prepared polymer for 10,000 steps period in the case: $c = 0.5, p_{\mathrm{d}} = 0.05$

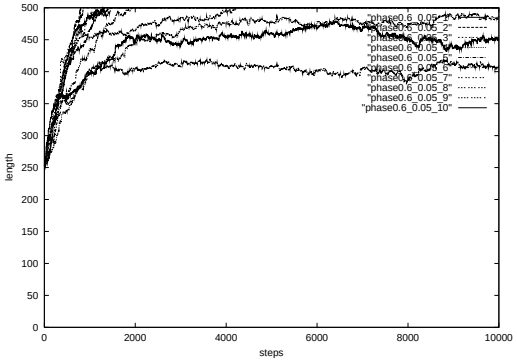

Figure 4.16: Time series of length of a prepared polymer for 10,000 steps period in the case: $c = 0.6, p_{\mathrm{d}} = 0.05$

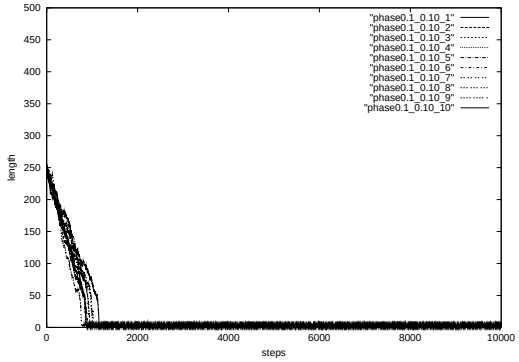

Figure 4.17: Time series of length of a prepared polymer for 10,000 steps period in the case: $c = 0.1, p_{\mathrm{d}} = 0.10$

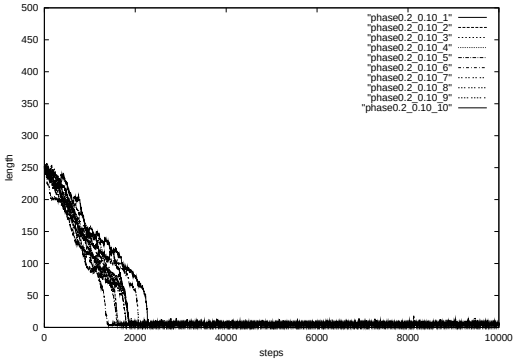

Figure 4.18: Time series of length of a prepared polymer for 10,000 steps period in the case: $c = 0.2, p_{\mathrm{d}} = 0.10$

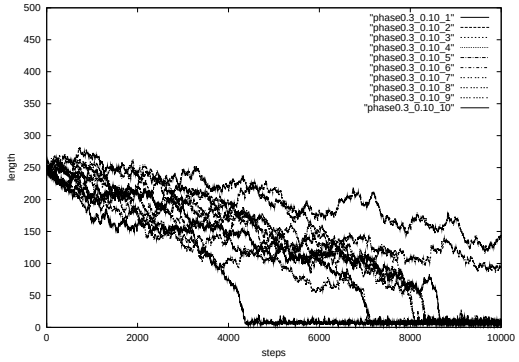

Figure 4.19: Time series of length of a prepared polymer for 10,000 steps period in the case: $c = 0.3, p_{\mathrm{d}} = 0.10$

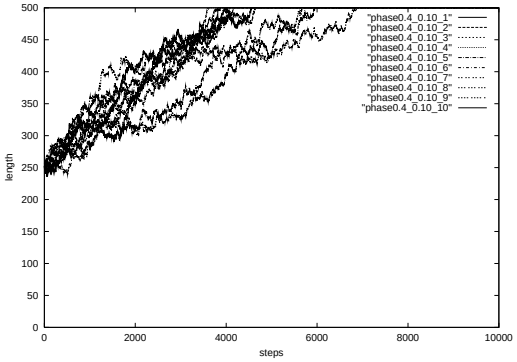

Figure 4.20: Time series of length of a prepared polymer for 10,000 steps period in the case: $c = 0.4, p_{\mathrm{d}} = 0.10$

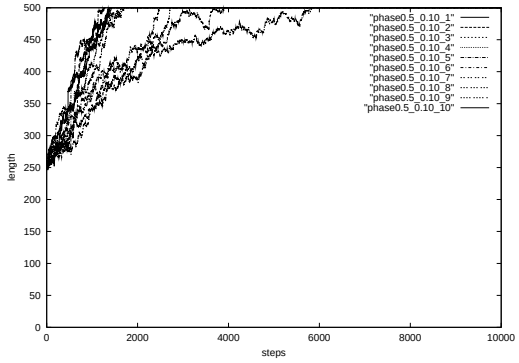

Figure 4.21: Time series of length of a prepared polymer for 10,000 steps period in the case: $c = 0.5, p_{\mathrm{d}} = 0.10$

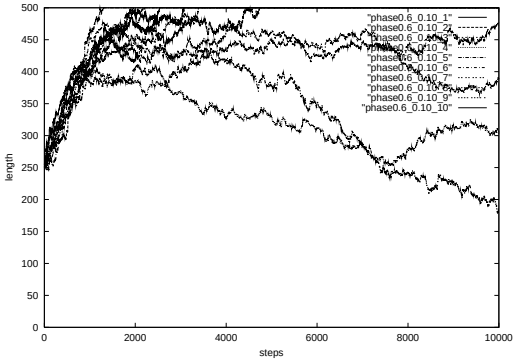

Figure 4.22: Time series of length of a prepared polymer for 10,000 steps period in the case: $c = 0.6, p_{\mathrm{d}} = 0.10$

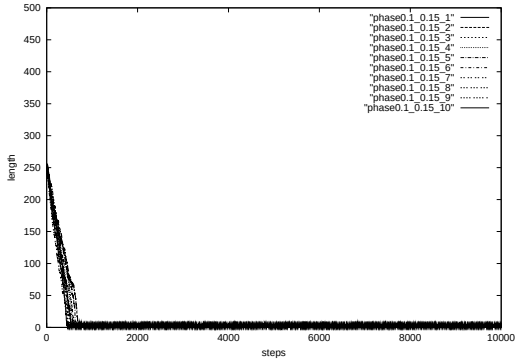

Figure 4.23: Time series of length of a prepared polymer for 10,000 steps period in the case: $c = 0.1, p_{\mathrm{d}} = 0.15$

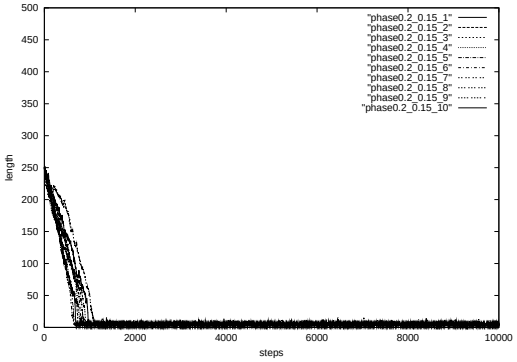

Figure 4.24: Time series of length of a prepared polymer for 10,000 steps period in the case: $c = 0.2, p_{\mathrm{d}} = 0.15$

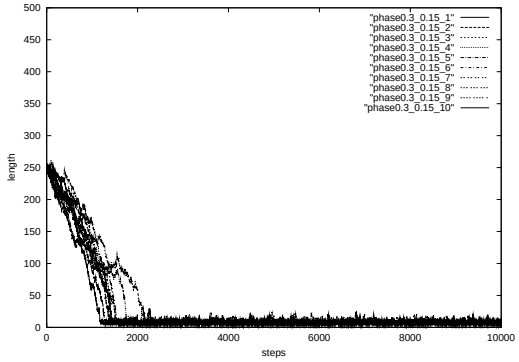

Figure 4.25: Time series of length of a prepared polymer for 10,000 steps period in the case: $c = 0.3, p_{\mathrm{d}} = 0.15$

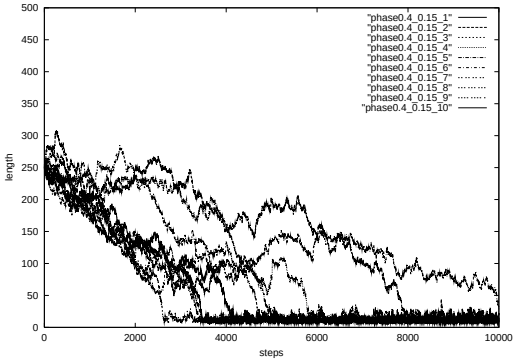

Figure 4.26: Time series of length of a prepared polymer for 10,000 steps period in the case: $c = 0.4, p_{\mathrm{d}} = 0.15$

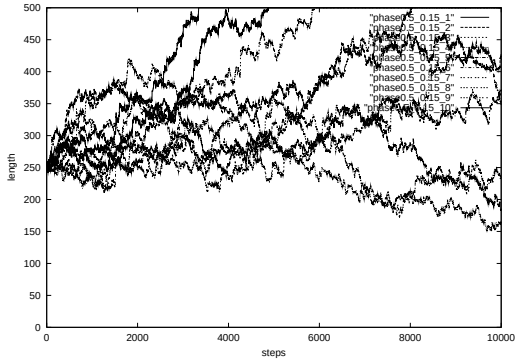

Figure 4.27: Time series of length of a prepared polymer for 10,000 steps period in the case: $c = 0.5, p_{\mathrm{d}} = 0.15$

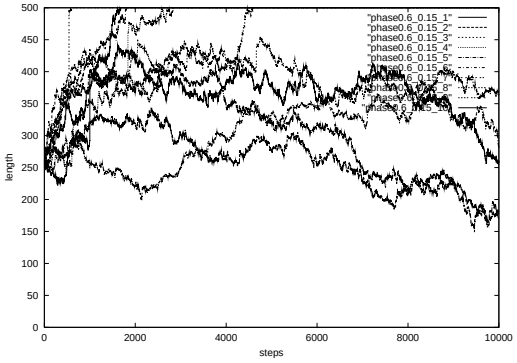

Figure 4.28: Time series of length of a prepared polymer for 10,000 steps period in the case: $c = 0.6, p_{\mathrm{d}} = 0.15$

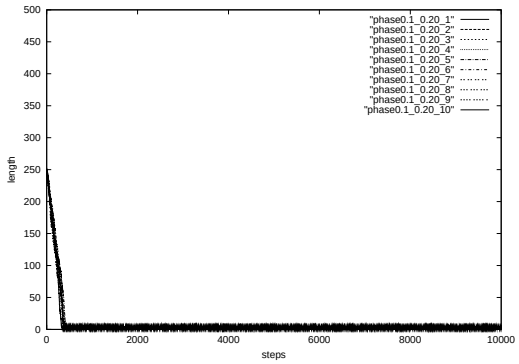

Figure 4.29: Time series of length of a prepared polymer for 10,000 steps period in the case: $c = 0.1, p_{\mathrm{d}} = 0.20$

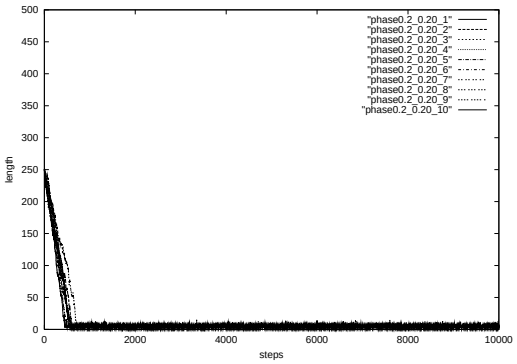

Figure 4.30: Time series of length of a prepared polymer for 10,000 steps period in the case: $c = 0.2, p_{\mathrm{d}} = 0.20$

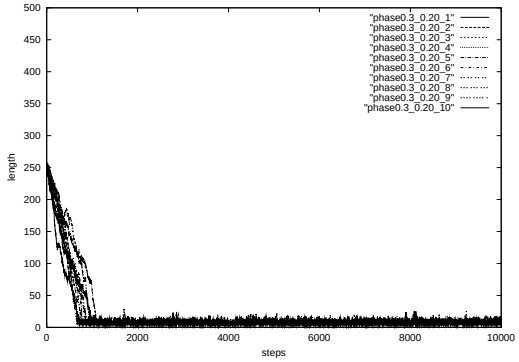

Figure 4.31: Time series of length of a prepared polymer for 10,000 steps period in the case: $c = 0.3, p_{\mathrm{d}} = 0.20$

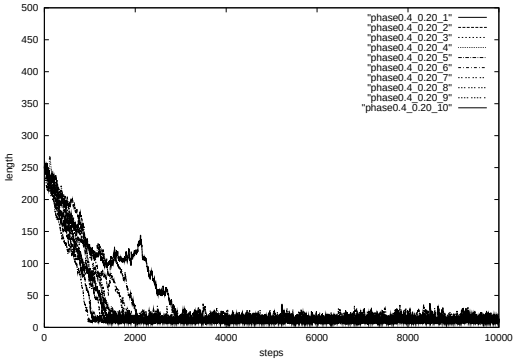

Figure 4.32: Time series of length of a prepared polymer for 10,000 steps period in the case: $c = 0.4, p_{\mathrm{d}} = 0.20$

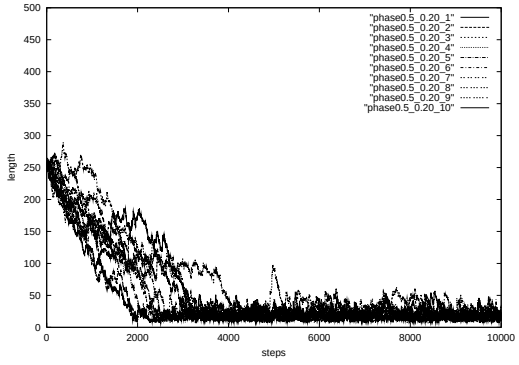

Figure 4.33: Time series of length of a prepared polymer for 10,000 steps period in the case: $c = 0.5, p_{\mathrm{d}} = 0.20$

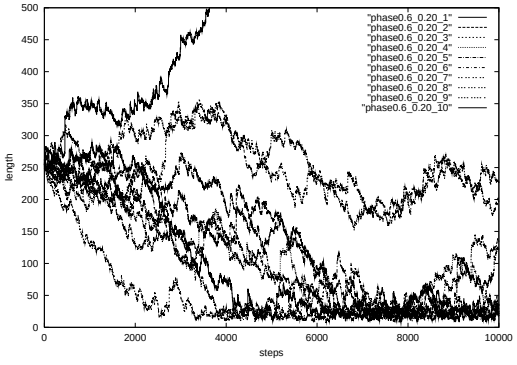

Figure 4.34: Time series of length of a prepared polymer for 10,000 steps period in the case: $c = 0.6, p_{\mathrm{d}} = 0.20$

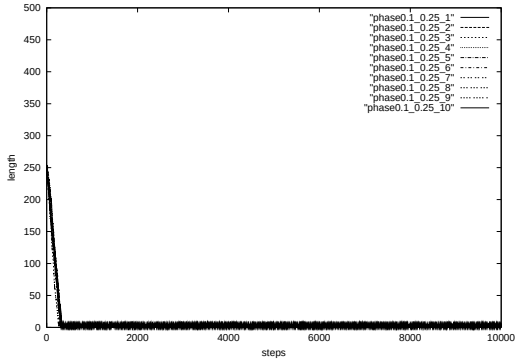

Figure 4.35: Time series of length of a prepared polymer for 10,000 steps period in the case: $c = 0.1, p_{\mathrm{d}} = 0.25$

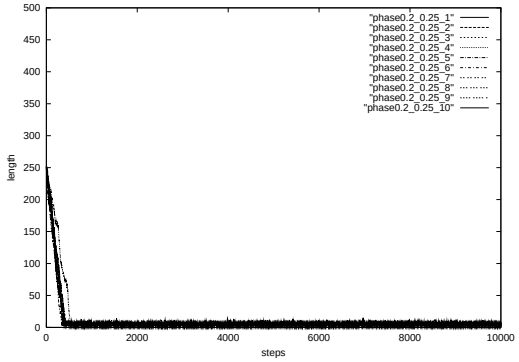

Figure 4.36: Time series of length of a prepared polymer for 10,000 steps period in the case: $c = 0.2, p_{\mathrm{d}} = 0.25$

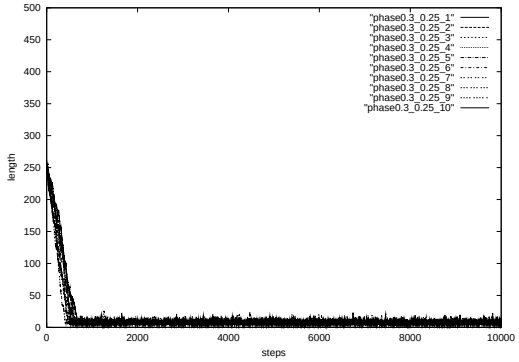

Figure 4.37: Time series of length of a prepared polymer for 10,000 steps period in the case: $c = 0.3, p_{\mathrm{d}} = 0.25$

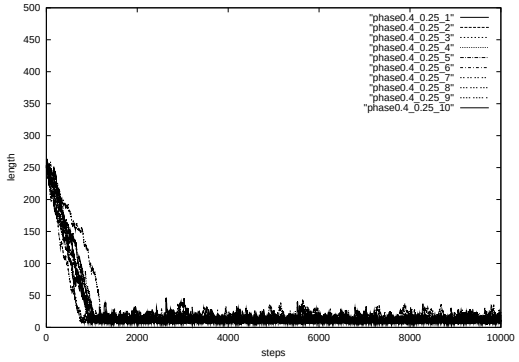

Figure 4.38: Time series of length of a prepared polymer for 10,000 steps period in the case: $c = 0.4, p_{\mathrm{d}} = 0.25$

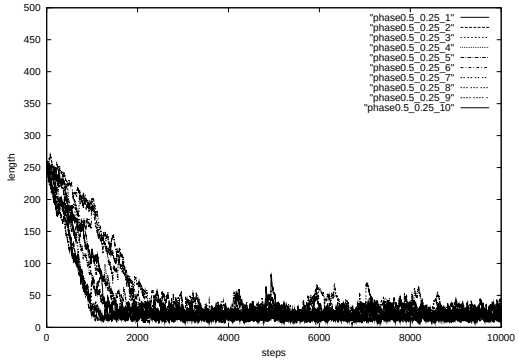

Figure 4.39: Time series of length of a prepared polymer for 10,000 steps period in the case: $c = 0.5, p_{\mathrm{d}} = 0.25$

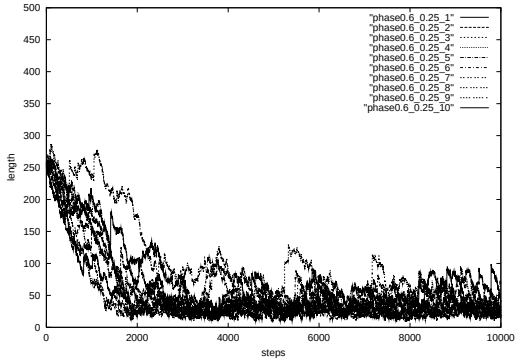

Figure 4.40: Time series of length of a prepared polymer for 10,000 steps period in the case: $c = 0.6, p_{\mathrm{d}} = 0.25$

until about 2,000 steps and then decrease till 10,000 steps. Also in the cases with $p_{\rm d} = 0.15$ $c = 0.1 \sim 0.6$ (shown in Figs.4.23–4.28), the behavior resembles those in the cases of $p_{\rm d} = 0.10$. The difference between these cases are the balancing concentration. In this case the concentration exists between $c = 0.4$ and $c = 0.5$.

And in two cases with $p_{\rm d} = 0.20$ $c = 0.1 \sim 0.6$ (shown in Figs.4.29–4.34) and $p_{\rm d} = 0.25$ $c = 0.1 \sim 0.6$ (shown in Figs.4.35–4.40), the figures show the shrinkage (except one case in Fig.4.40). These things mean that the detach probabilities are so large that the net growth couldn't occur in these cases.

Next I calculate the mean growth/shrinkage velocity in all the above cases in Fig.4.41 and show the contour plot in Fig.4.42.

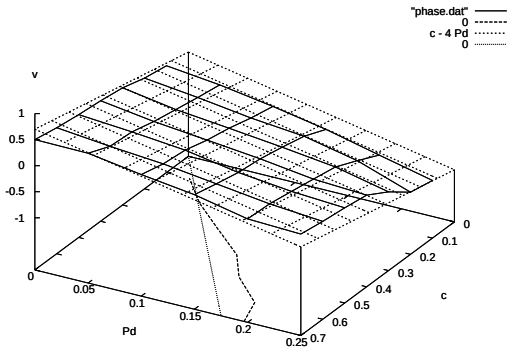

Figure 4.41: Mean growth/shrinkage velocity in possible cases in the lattice polymerization model without the internal state dynamics. System size: $X = 500, Y = 250$. Parameter $l_{\rm th} = 10$. Steps: 10,000. The curve on the base stands for the zero mean growth/shrinkage velocity in the lattice polymerization model and the line on the base stands for the zero mean growth/shrinkage velocity calculated by the equation: $v = c - 4p_{\rm d}$

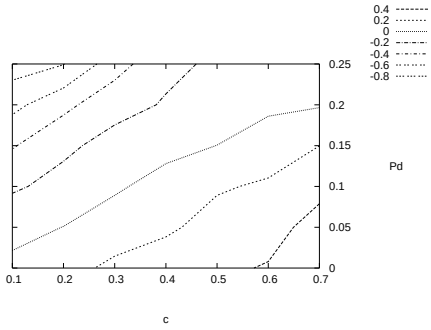

Figure 4.42: Contour plot of the mean growth/shrinkage velocity in possible cases in the lattice polymerization model without the internal state dynamics. System size: $X = 500, Y = 250$. Parameter $l_{\rm th} = 10$. Steps: 10,000.

In the low concentration region $c \sim 0.1$, the growth/shrinkage velocity is fitted by the next equation,

$$v = c - 4p_{\rm d} \tag{4.1}$$

This equation is derived by the next speculation. To think the one lattice site of

the end of polymer combined with the other end, the probability of transfer into this site is given by the concentration c and the probability of transfer from this site to the nearest neighbor sites is given by the detach probability $p_{\rm d}$ times the number of the nearest neighbor sites 4 i.e. $4p_{\rm d}$. So the net growth/shrinkage velocity becomes eq.4.1.

In the region with the concentration $c > 0.3$ and the detach probability near 0.25, the absolute value of the mean shrinkage velocity become smaller than those derived from eq.4.1. I speculate that these thing occur because the motion of detached monomers are suppressed by the exclusive volume effect.

Also the region with the concentration $c > 0.3$ and the detach probability near 0, the values of the mean growth velocity become smaller, too. I speculate that the many polymer nucleate in these region so that many monomers add to such a polymer.

The zero growth/shrinkage velocity of the lattice model in the large concentration region is shifted from the line derived from eg.4.1. The effective volume effect would make the above thing.

Here I discuss briefly the role of the internal state dynamics. In the model without the internal state dynamics, we see a sharp critical concentration for the growth/shrinkage. The effect of the internal state dynamics may blur the critical concentration to a finite range so that it helps to grow the polymer at a smaller concentration. This implies that the internal state dynamics plays a very important role to the state different from equilibrium.

4.2 Shifted peak of length distribution in the lattice polymerization model without the internal state dynamics

I found some kind of shifted peak in the length distribution of linear polymers which are longer than the threshold length in the lattice polymerization model without (c)internal state change.

To understand both the microscopic and the macroscopic behavior accurately, I have proposed a lattice polymerization model for the dynamics of cytoskeletal fila-

ments [26, 27] . The model consists of N subunits in a volume of V sites. This model has three essential ingredients: (a) random motion of subunits in space, (b) short range interaction between subunits with a threshold length, and (c) internal state dynamics of each subunit. This model reveals a characteristic phenomena mimicking the *dynamic instability* observed in real microtubules *in vivo* [3] and *in vitro* [1, 22] in which a single microtubule alternates show growths and rapid shrinkage of its length.

I show the shift peak of the length distribution of a single filament to the right (longer direction) (shown in Fig.4.43).

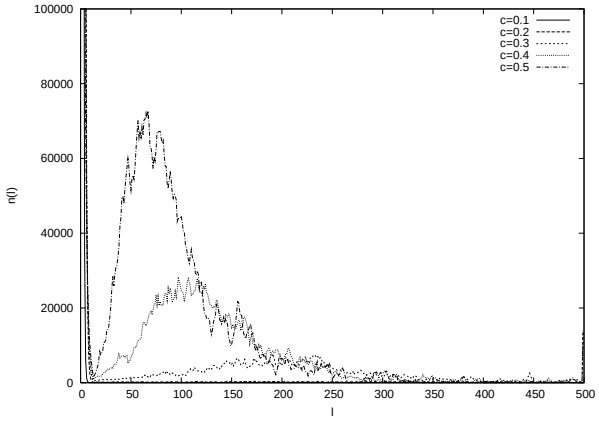

Figure 4.43: Length Distribution of cytoskeletal filaments in several subunit numbers $N = 12,500,\ 25,000,\ 37,500,\ 50,000,\ 62,500$ which correspond to the concentration $c = N/V = 0.1,\ 0.2,\ 0.3,\ 0.4,\ 0.5$ for 10,000 steps period in a lattice polymerization model. l stands for the length of a filament. $n(l)$ stands for the filaments' number of length l. This figure shows an area of number: $0 \leq n(l) \leq 100,000$

This phenomena would take place only in the non-equilibrium steady state and cannot be explained in the conventional polymerization kinetics [10] which considers the conservation of total number of subunits in the section of the equilibrium theory but doesn't consider it in the section of the kinetic theory. It's important to treat the monomer number explicitly like Oosawa *et al.* [7]. So I construct an effective kinetic model for polymerization with a threshold length in a finite volume system (see the chapter III).

4.2.1 Length distribution of polymers with length l in the effective kinetic model

I calculate the length distribution of polymers with length l in several initial concentrations c_0 for the threshold length $l_{\rm th} = 1, 3, 5, 10$ with the maximum length $L = 5,000$ in the finite volume $V = 10^{10}$ numerically. I show the results in Fig.4.44-4.47 at 100,000 steps.

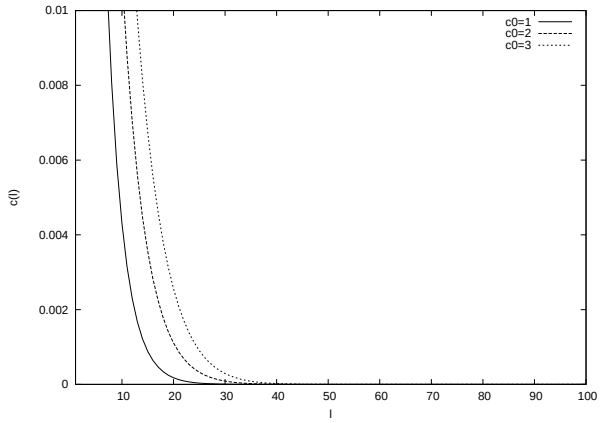

Figure 4.44: The length distribution of polymers with the threshold length $l_{\rm th} = 1$ with the maximum length $L = 5,000$ in the volume $V = 10^{10}$ at 100,000 steps with parameters: $k_m^{\rm on} = k_m^{\rm off} = k_p^{\rm on} = 0.1, k_p^{\rm off} = 0.001$. l stands for the length and c_l stands for the concentration of polymers with length l. $c_0 = 1, 2, 3$ stand for the concentration parameters. This figure shows the area of number: $0 \leq n_l \leq 100$ and the concentration: $0 \leq c_l \leq 0.01$

.

Fig.4.44 corresponds to the case of the simple polymerization i.e. the case without nucleation because the threshold length is 1 and all the kinetic constants of polymer with length l are the same value. The figure shows the exponential decay.

From the results in the case of $c_0 = 3$ in Fig.4.45 and in all the cases in Fig.4.46 and Fig.4.47, I found the shifted peaks of the length distribution over the threshold lengths. To understand the cause of this shifted peaks, I calculate the time evolution of the length distribution of the threshold length $l_{\rm th} = 5$ for 200,000 steps periods. I show the result in Fig.4.48

From Fig.4.48, I found the relaxation of the shifted peak with time. I speculate that the some polymers after nucleation grow more longer and the other polymers

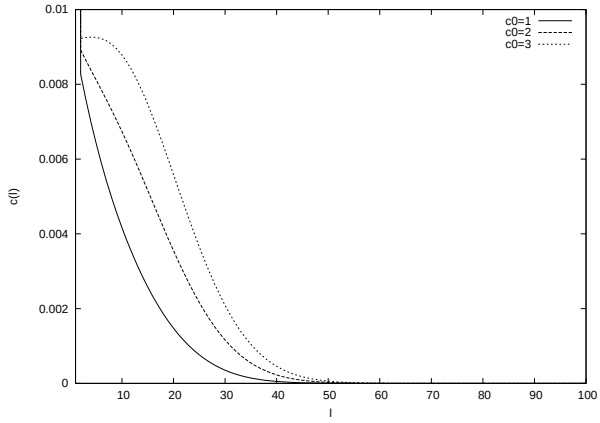

Figure 4.45: The length distribution of polymers with the threshold length $l_{\rm th} = 3$ with the maximum length $L = 5,000$ in the volume $V = 10^{10}$ at 100,000 steps with parameters: $k_m^{\rm on} = k_m^{\rm off} = k_p^{\rm on} = 0.1, k_p^{\rm off} = 0.001$. l stands for the length and c_l stands for the concentration of polymers with length l. $c_0 = 1, 2, 3$ stand for the concentration parameters. This figure shows the area of number: $0 \leq n_l \leq 100$ and the concentration: $0 \leq c_l \leq 0.01$

.

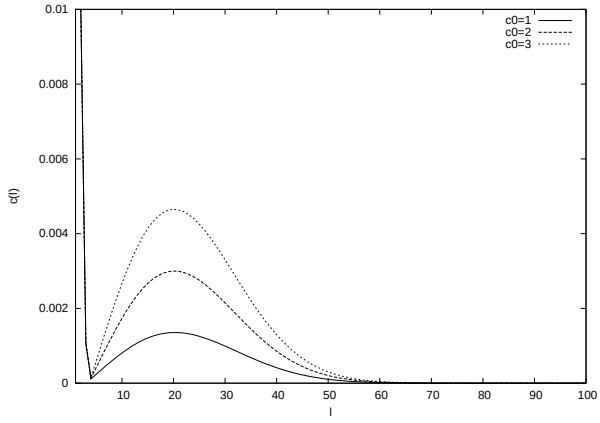

Figure 4.46: The length distribution of polymers with the threshold length $l_{\rm th} = 5$ with the maximum length $L = 5,000$ in the volume $V = 10^{10}$ at 100,000 steps with parameters: $k_m^{\rm on} = k_m^{\rm off} = k_p^{\rm on} = 0.1, k_p^{\rm off} = 0.001$. l stands for the length and c_l stands for the concentration of polymers with length l. $c_0 = 1, 2, 3$ stand for the concentration parameters. This figure shows the area of number: $0 \leq n_l \leq 100$ and the concentration: $0 \leq c_l \leq 0.01$

.

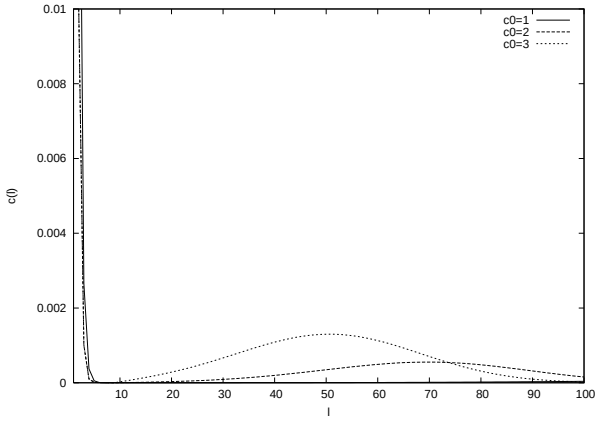

Figure 4.47: The length distribution of polymers with the threshold length $l_{\rm th} = 10$ with the maximum length $L = 5,000$ in the volume $V = 10^{10}$ at 100,000 steps with parameters: $k_m^{\rm on} = k_m^{\rm off} = k_p^{\rm on} = 0.1, k_p^{\rm off} = 0.001$. l stands for the length and c_l stands for the concentration of polymers with length l. $c_0 = 1, 2, 3$ stand for the concentration parameters. This figure shows the area of number: $0 \leq n_l \leq 100$ and the concentration: $0 \leq c_l \leq 0.01$

.

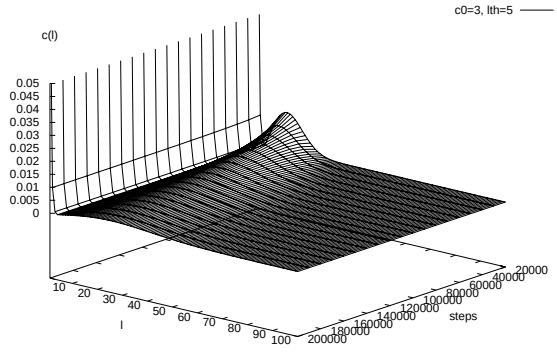

Figure 4.48: The time evolution of the length distribution of polymers with the threshold length $l_{\rm th} = 5$ with the maximum length $L = 5,000$ in the volume $V = 10^{10}$ for 200,000 steps periods with parameters: $k_m^{\rm on} = k_m^{\rm off} = k_p^{\rm on} = 0.1, k_p^{\rm off} = 0.001$. l stands for the length and c_l stands for the concentration of polymers with length l. $c_0 = 1, 2, 3$ stand for the concentration parameters. The word "steps" stands for the steps in the calculation. This figure shows the area of number: $0 \leq n_l \leq 100$ and the concentration: $0 \leq c_l \leq 0.01$

.

vanish in our effective kinetic model. This speculation is reasonable in the real phenomena. In the nucleation phase, abundant nuclei are created and some of them could grow more longer. By the advance of technology these abundant nuclei in the nucleation phase could be observed in the nucleation phase in the future.

4.2.2 Time evolution of the average length of polymers

Next I analyze the time evolution of the average length $\langle l \rangle$ of polymers and that of the monomer concentration for different threshold lengths $l_{\rm th} = 2, 3, 4, 5$ in order to understand the behavior of the length distribution. I show the result of the time evolution of the average length $\langle l \rangle$ in Fig.4.49.

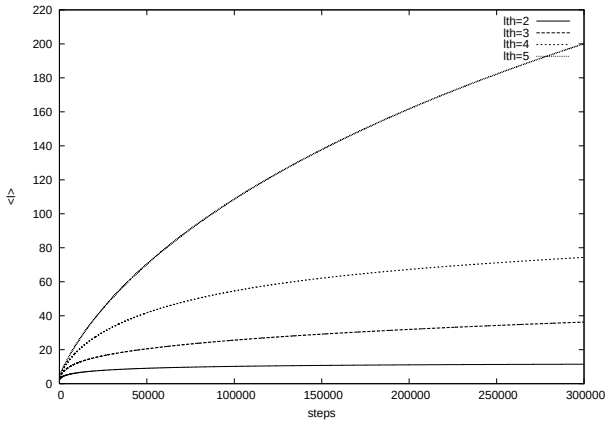

Figure 4.49: The time evolution of the average length of polymers with the threshold length $l_{\rm th} = 2, 3, 4, 5$ with the maximum length $L = 5,000$ in the volume $V = 10^{10}$ for 300,000 steps periods with parameters: $k_m^{\rm on} = k_m^{\rm off} = k_p^{\rm on} = 0.1, k_p^{\rm off} = 0.001 c_0 = 1$. $\langle l \rangle$ stands for the average length of polymers. The word "steps" stands for the steps in the calculation. This figure shows the area of : $0 \leq \langle l \rangle \leq 220$

.

We could see that the average length of polymers are so sensitive to the threshold length in Fig.4.49. I plot the dependence of the average length of polymers on the threshold length at 300,000 steps in Fig.4.50. The average length of polymers depends on the threshold length exponentially.

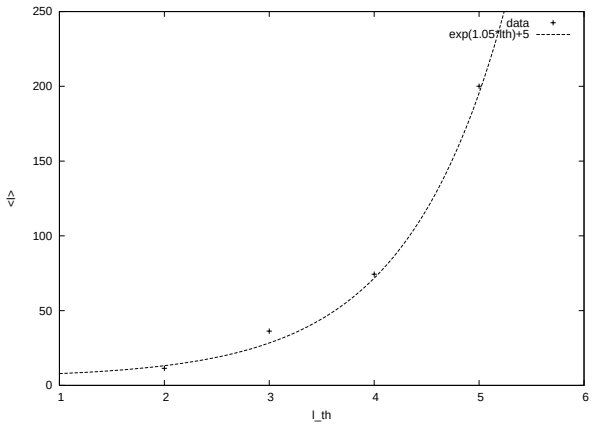

Figure 4.50: The dependence of the average length of polymers on the threshold length at 300,000 steps with the maximum length $L = 5,000$ in the volume $V = 10^{10}$ at 300,000 steps with parameters: $k_m^{\rm on} = k_m^{\rm off} = k_p^{\rm on} = 0.1, k_p^{\rm off} = 0.001 c_0 = 1$. ¡$l$¿ stands for the average length of polymers. The word 'steps' stands for the steps in the calculation. This figure shows the area of : $0 \leq \langle l \rangle \leq 250$

.

4.3 Time relaxation of the monomer concentration

I show the time relaxation of the monomer concentration in Fig.4.51. The behavior of the time relaxation becomes almost two step processes which decay exponentially depending on the $k_m^{\rm on}$ and $k_p^{\rm on}$.

Summary

I construct a effective kinetic model for the linear polymerization with a threshold in a finite volume system treating the monomer number explicitly. This effective model shows the shifted peaks of the distribution with several threshold lengths $l_{\rm th} = 1, 3, 5, 10$ in several concentration ($c_0 = 1, 2, 3$) like the distribution simulated in our lattice polymerization model. I calculate the time evolution of the distribution with a threshold $l_{\rm th} = 5$ for 200,000 steps periods. I found the relaxation of the shifted peak. And I analyze the average lengths of polymers with threshold lengths $l_{\rm th} = 2, 3, 4, 5$ which are so sensitive to the threshold lengths. I also calculate the time relaxations of the monomer concentration with threshold lengths $l_{\rm th} = 2, 3, 4, 5$ those behavior show the two step processes which decay exponentially depending on

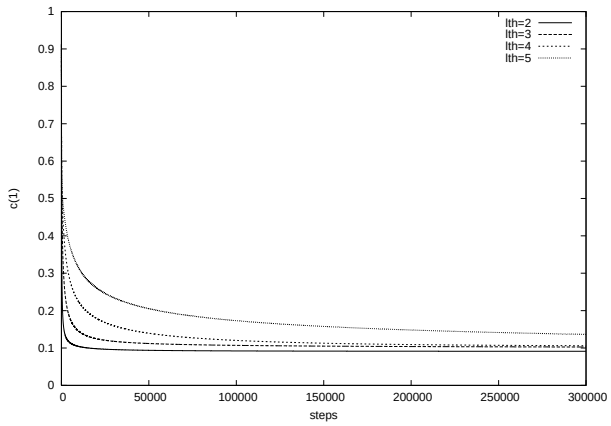

Figure 4.51: The time relaxation of the monomer concentration with the threshold length $l_{\rm th} = 2, 3, 4, 5$ with the maximum length $L = 5,000$ in the volume $V = 10^{10}$ for 300,000 steps periods with parameters: $k_m^{\rm on} = k_m^{\rm off} = k_p^{\rm on} = 0.1, k_p^{\rm off} = 0.001 c_0 = 1$. $c(1)$ stands for the monomer concentration. The word "steps" stands for the steps in the calculation. This figure shows the area of : $0 \leq \langle l \rangle \leq 250$.

the $k_m^{\rm on}$ and $k_p^{\rm on}$.

This new simple kinetic model has an important meaning for the non equilibrium state in a finite volume system, because this model could treat the monomer number explicitly i.e. finite source system that is different from the conventional subunit bath system i.e. infinite source system.

Chapter 5

Results II: a model with internal state dynamics

I have examined the lattice polymerization model numerically in stochastic simulations. I have investigated statistical behavior of samples containing many tubulin dimers.

5.1 Dynamic instability in the lattice polymerization model

In order to investigate the properties of phenomena like a dynamic instability, I prepare a nucleus in the system and I trace the dynamics of the prepared nucleus thereafter. The result shows many characteristics observed in experiments. Among them, cytoskeletal filaments in this model perform oscillatory behavior resembling the observed phenomena of dynamic instability as shown in Fig.5.1 where l stands for the length of a prepared filament. In this case, the velocity of growth is about 50×8 nm/1000 steps, which corresponds to about 24 μ/min if estimated by using the value 0.2 $\times10^{-14}$ m^2/sec of the diffusion constant in the case where a spherical particle of 8 nm long and 55 kilodaltons exists in water. In actual experiments, the typical velocities of growth is observed to be about 2 μ/min (50 dimers/sec), while the velocities of shortening are 10 times faster [6]. In our simulation, this velocity becomes of the same order under a suitable set of parameters.

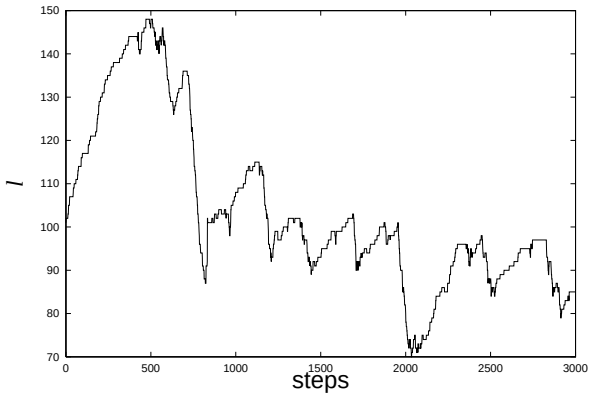

Figure 5.1: Time series of the degree of polymerization over 3000 steps period.

Discussion

At this stage this model is somewhat artificial, but as a first step, to construct such a toy model of a system of many protein molecules is really invaluable for understanding the phenomena in biological cells quantitatively. Such a model is expected to fill the gap between the microscopic models based on the atomic behavior and the macroscopic thermodynamic or chemical kinetic models.

5.2 A critical concentration in the lattice polymerization model

In each simulation, I prepare a cytoskeletal filament in a system and observe its length l over 10,000 steps in order to investigate the growth-shrinkage dynamics especially the *dynamic instability*. Fig.5.2 shows a snapshot of a simulation at 100 steps.

In order to investigate the dependence of the dynamics on concentrations, I performed a series of simulations with this model for $l_{\rm th} = 50$, $\tau_{\rm d} = 250$, $\tau_D = -\tau_T = 300$, $(X = 300, Y = 100)$, at relatively low concentrations $c = 0.05$, 0.0625, 0.75, 0.0875, 0.1, corresponding respectively to $\tau_{\rm a} = 20$, 16, 13.3, 11.4, 10, over 10,000 steps periods and calculate the length of the cytoskeleton prepared with the length of $l = 200$; some of the results are shown in Figs.5.3 to 5.5. These figures show that the growth velocity averaged over long time interval increase with concentration. Fig.5.3 shows

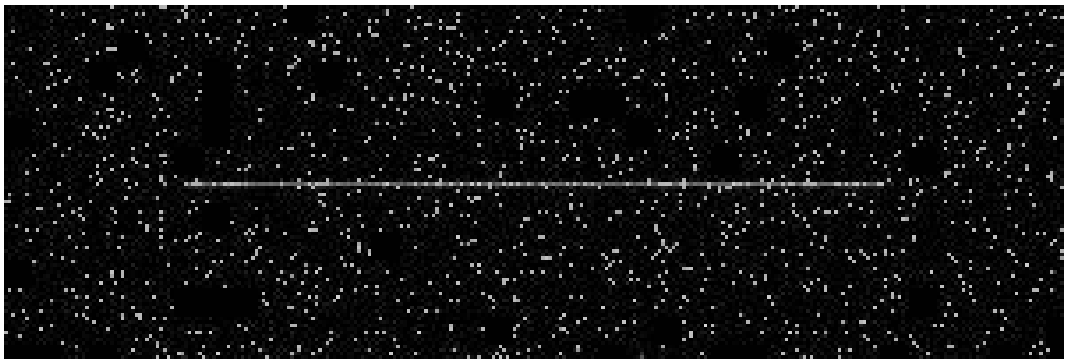

Figure 5.2: Snapshot of a simulation at 100 steps. Parameters: $l_{\rm th} = 50$, $\tau_{\rm d} = 250$, $\tau_D = -\tau_T = 300$, $c = 0.05$ *i.e.* $\tau_{\rm a} = 20$, ($X = 300$, $Y = 100$). There prepared a cytoskeleton whose length is 200 and it is located in the center of the lattice in the horizontal direction. Gray square and White square stand for **D** state and **T** state particles' sites severally.

that for $c = 0.05$ the prepared chain of cytoskeleton is depolymerizing; polymers are not stabilized in the equilibrium state. I calculate the mean long-time velocity $v_{\rm long}$, which is defined as the slope of the linear regression. The relation between the mean long-time velocity $v_{\rm long}$ and the concentration c are shown in Fig.5.8 and the average values of $v_{\rm long}$ in each concentration are connected with lines as a guide for the eyes. It is considered that the curve which connects these points crosses the line $v_{\rm long} = 0$ at the concentration c_0 at around 0.065. This suggests that there exists a *critical concentration* of polymerizations, for this set of parameters so that the growth-shrinkage dynamics continues for a long time without essential change of the length around the concentration near c_0. This concentration c_0 does not coincides with the critical concentration for the growth to initiate[**?**].

5.3 Probability distribution function of the short-time average velocity of the length in the lattice polymerization model

Next I analyze the time series data for $l_{\rm th} = 50, \tau_{\rm d} = 250, \tau_{\rm D} = -\tau_{\rm T} = 300$, ($X = 300, Y = 100$), at the concentration c =0.0625 nearest to c_0. The simulation is done 20 times for different random numbers each starting from $l = 200$. As is expected

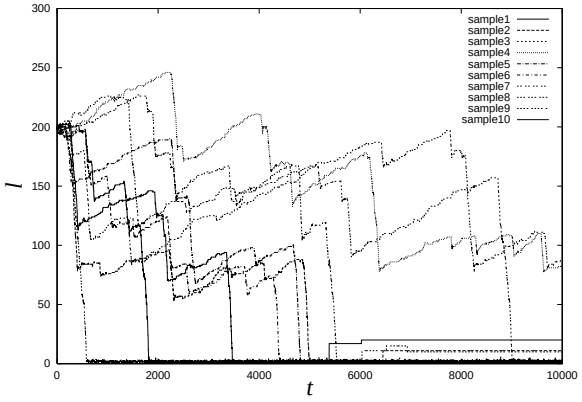

Figure 5.3: $c = 0.05$ *i.e.* $\tau_{\mathrm{a}} = 20$

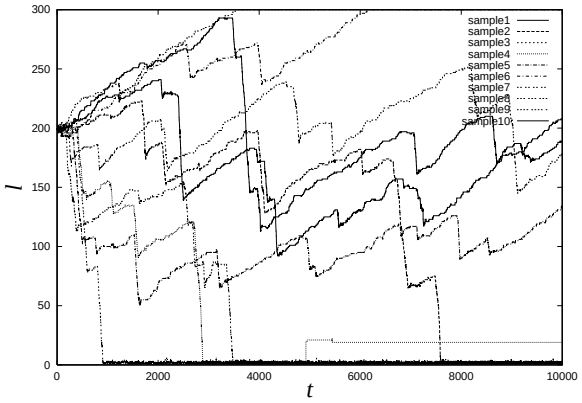

Figure 5.4: $c = 0.0625$ *i.e.* $\tau_{\mathrm{a}} = 16$

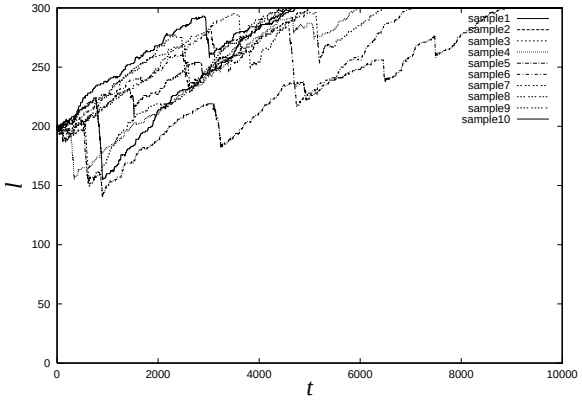

Figure 5.5: $c = 0.075$ *i.e.* $\tau_{\mathrm{a}} = 13.3$

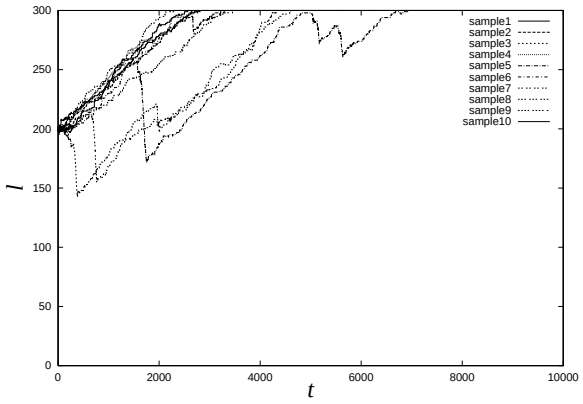

Figure 5.6: $c = 0.0875$ *i.e.* $\tau_{\mathrm{a}} = 11.4$

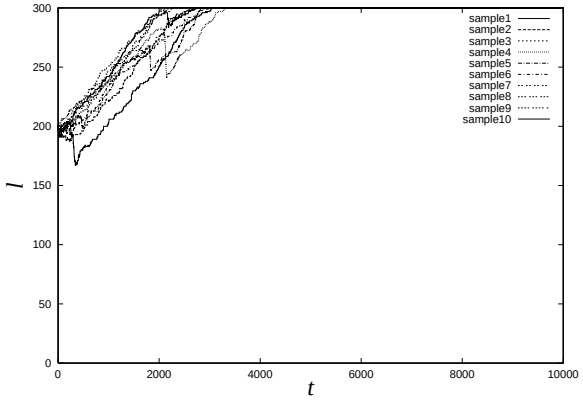

Figure 5.7: $c = 0.1$ *i.e.* $\tau_{\mathrm{a}} = 10$

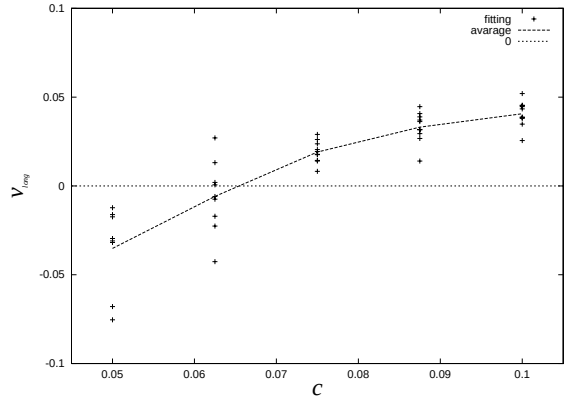

Figure 5.8: Mean long-time velocity v_{long} vs. Concentration c and the averaged curve of v_{long}

it shows a lasting dynamic instability as seen in Fig.5.9 where three samples of the length change are displayed. From these results, I calculate the mean velocity over several time intervals $\triangle t$: $v = \triangle l/\triangle t$. Fig.5.10 shows the time series of the velocity $v_{\rm short}$ over a short time intervals $\triangle t = 100$. It has observed in real experiments that the growth velocity is smaller than the shrinkage velocity in the order of 10. The time series of the velocity in Fig.5.10 has a small velocity component in positive region and some large velocity components in negative region.

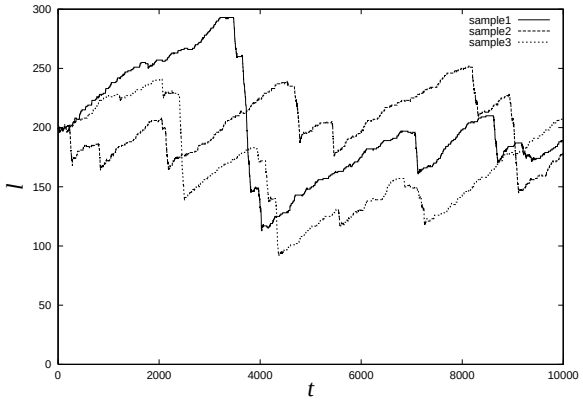

Figure 5.9: Time series of the length of one cytoskeleton over 10,000 steps period. l and t stand for the length and steps severally.

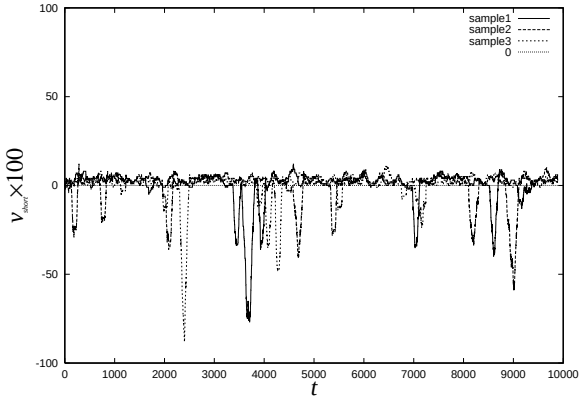

Figure 5.10: Time series of the velocity of one cytoskeletons' length over 10,000 steps period. $v_{\rm short}$ and t stand for the velocity and steps respectively. $v_{\rm short} = \triangle l/\triangle t$ (here $\triangle t = 100$)

I show the probability distribution functions (PDFs) of the velocity with some time lags in Fig.5.11 over 10,000 steps periods for 20 trials with the time lag $\triangle t$ from

100 steps to 1,000 steps. Each curve of PDF has a shoulder at around $v_{\rm short} = 0$ and a peak at around 0.02 and has the lower tail longer than the upper tail for large $\triangle t$. The central part of the PDF of the length change $\triangle l$ widen linearly with the time lags $\triangle t$ so that the central part of the PDFs of the velocity do not essentially depend on $\triangle t$.

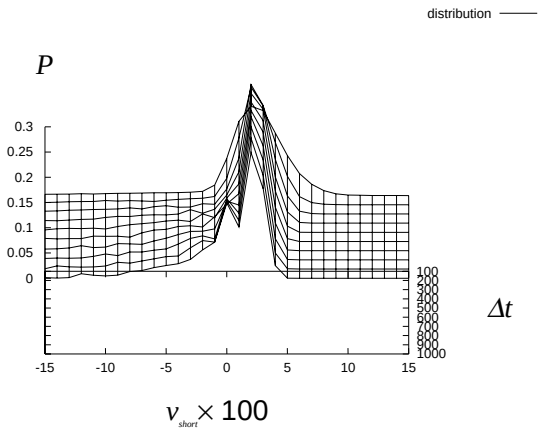

Figure 5.11: Probability distribution functions of the mean short-time velocity.

Summary

Using our lattice model of cytoskeletons I analyze the behavior of linear polymers made out of proteins which are continually polymerizing and depolymerizing in the square lattice of 300×100 with the set of parameters: $l_{\rm th} = 50, \tau_{\rm d} = 250, \tau_{\rm D} = -\tau_{\rm T} = 300$. I observed that subunits of cytoskeleton do not polymerize in equilibrium at very low concentrations. The analysis of the long-time velocity shows that there exists a *critical concentration* of polymerizations in cytoskeletons' dynamics for the above set of parameters at around $c = 0.065$. I also observed the phenomena with slow growth and rapid shrinkage which are characteristic of the *dynamic instability*. I calculate the probability distribution functions of the short-time velocity, which has a shoulder and a peak and also a long lower tail. The central part of the distribution is essentially invariant of the time lag $\triangle t$.

Chapter 6

Summary

In this thesis, I introduce a lattice polymerization model for the dynamics of cytoskeletal filaments including physical ingredients of (a) random motion in space, (b) short range interaction with a threshold length, and (c) internal state variable and I also introduce an effective kinetic model for linear polymerization with a threshold length in a finite volume system.

I perform simulations of the lattice polymerization model in two limiting cases of a diffusion-limited aggregation model and a simple lattice gas model. These cases show important features in the cytoskeletons' dynamics: in low concentrations, the growth velocity of a polymer increases linearly as the concentration increases, while the shrinkage velocity of a polymer mainly depends on the detach probability. These results will be important for the understanding of the growth-shrinkage dynamics of cytoskeletons such as dynamic instability.

In DLA, the both ends of polymer may be considered to be sinks of subunits. The problem of diffusion with a sink is described by the Laplace equation in the stationary state. A basic solution in two dimensions is expressed by $c(r) = a \log(r/r_0)$, where c is concentration, r is distance from the sink and a and r_0 are constants. The six nearest neighbor sites have a effective concentration $c_{\rm eff}$ then the growth velocity should be $\bar{v_{\rm g}} = (6/4)c_{\rm eff}$. I estimate by using the simulation result of $\bar{v_{\rm g}} = 0.45c$ that the concentration reaches the uniform value at the distance of about $r \sim 10$ sites. This estimation is based on the idea that the both ends of polymer grow up slowly by the diffusion with the logarithmic distribution of concentration around the ends.

In the simulations of LGM, I found that the shrinkage velocity is determined essen-

tially by the detach probability. The both ends of polymer are the source of subunits in contrast to DLA. Applying a similar argument as above with sinks replaced by sources, I estimate that at the distance of about $r \sim 3$ sites the concentration reaches the uniform value, though in this case the process may not be stationary due to the large shrinkage velocity of $\bar{v}_{\rm s} \simeq -1$.

I discuss briefly the role of the internal state dynamics. In the model without the internal state dynamics, I have a sharp critical concentration for the growth/shrinkage. The effect of the internal state dynamics may blur the critical concentration to a finite range so that it helps to grow the polymer at a smaller concentration. This implies that the internal state dynamics plays a very important role to the state different from equilibrium.

I construct a effective kinetic model for the linear polymerization with a threshold in a finite volume system treating the monomer number explicitly. This effective model shows the shifted peaks of the distribution with several threshold lengths $l_{\rm th} = 1, 3, 5, 10$ in several concentration ($c_o = 1, 2, 3$) like the distribution simulated in our lattice polymerization model. I calculate the time evolution of the distribution with a threshold $l_{\rm th} = 5$ for 200,000 steps periods. I found the relaxation of the shifted peak. And I analyze the average lengths of polymers with threshold lengths $l_{\rm th} = 2, 3, 4, 5$ which are so sensitive to the threshold lengths. I also calculate the time relaxations of the monomer concentration with threshold lengths $l_{\rm th} = 2, 3, 4, 5$ those behavior show the two step processes which decay exponentially depending on the $k_m^{\rm on}$ and $k_p^{\rm on}$.

This new simple kinetic model has an important meaning for the non equilibrium state in a finite volume system, because this model could treat the monomer number explicitly i.e. finite source system that is different from the conventional subunit bath system i.e. infinite source system.

I found some kind of shifted peak in the length distribution of linear polymers which are longer than the threshold length in the lattice polymerization model without (c)internal state change.

Also in order to investigate the properties of phenomena like a dynamic instability, I prepare a nucleus in the system and I trace the dynamics of the prepared nucleus

thereafter. The result shows many characteristics observed in experiments. Among them, cytoskeletal filaments in this model perform oscillatory behavior resembling the observed phenomena of dynamic instability.

Using our lattice model of cytoskeletons I analyze the behavior of linear polymers made out of proteins which are continually polymerizing and depolymerizing in the square lattice of 300×100 with the set of parameters: $l_{\rm th} = 50, \tau_{\rm d} = 250, \tau_{\rm D} = -\tau_{\rm T} = 300$. I observed that subunits of cytoskeleton do not polymerize in equilibrium at very low concentrations. The analysis of the long-time velocity shows that there exists a *critical concentration* of polymerizations in cytoskeletons' dynamics for the above set of parameters at around $c = 0.065$. I also observed the phenomena with slow growth and rapid shrinkage which are characteristic of the *dynamic instability*. I calculate the probability distribution functions of the short-time velocity, which has a shoulder and a peak and also a long lower tail. The central part of the distribution is essentially invariant of the time lag $\triangle t$.

The lattice model and the kinetic model is somewhat artificial but important for the understanding of cellular process and the nature of cytoskeletal proteins.

Appendix A

Two mathematical relations

In this appendix, I prove two simple mathematical relations which is used in the Oosawa's theory.

If x is a positive number (< 1), then the next two mathematical relations are approved.

$$\sum_{i=0}^{\infty} x^i = \frac{1}{1-x} \tag{A.1}$$

and

$$\sum_{i=0}^{\infty} ix^i = \frac{x}{(1-x)^2}. \tag{A.2}$$

These mathematical relations are easy to prove. I call the infinite sum in eq.(A.1) S. Then,

$$S = 1 + x + x^2 + ... \tag{A.3}$$

$$xS = x + x^2 + x^3 + ... \tag{A.4}$$

I sum up the above two equations (A.3) and (A.4),

$$S = \sum_{i=0}^{\infty} x^i = \frac{1}{1-x} \tag{A.5}$$

And i take the x-derivative of S,

$$S' = 1 + 2x + 3x^2 + ... \tag{A.6}$$

Then,

$$xS' = x + 2x^2 + 3x^3 + ... = \sum_{i=0}^{\infty} ix^i = \frac{x}{(1-x)^2}. \tag{A.7}$$

Appendix B

Law of mass action and Linear response coefficient

In this appendix, I consider the linear response theory in the chemical reaction and derive the law of mass action [33] and the linear response coefficient in the reaction.

I consider a chemical reaction expressed as following,

$$\mathrm{A} + \mathrm{B} \underset{k^{\mathrm{off}}}{\overset{k^{\mathrm{on}}}{\rightleftharpoons}} \mathrm{C} + \mathrm{D}, \tag{B.1}$$

where k^{on} and k^{off} stands for the rate constants of the association and dissociation, respectively. I assume the molecular concentrations of A,B,C,D as $c_{\mathrm{A}}, c_{\mathrm{B}}, c_{\mathrm{C}}, c_{\mathrm{D}}$,respectively and the kinetic equation for c_{A} is expressed as below,

$$\frac{dc_{\mathrm{A}}}{dt} = -k^{\mathrm{on}} c_{\mathrm{A}} c_{\mathrm{B}} + k^{\mathrm{off}} c_{\mathrm{C}} c_{\mathrm{D}}. \tag{B.2}$$

For the species B,C,D, the kinetic equations are like the above equation. In the equilibrium state, if I assume the solution of these equations as $c_{\mathrm{A}}^{\mathrm{eq}}, c_{\mathrm{B}}^{\mathrm{eq}}, c_{\mathrm{C}}^{\mathrm{eq}}, c_{\mathrm{D}}^{\mathrm{eq}}$, the kinetic equation for c_{A} becomes as below,

$$\frac{dc_{\mathrm{A}}}{dt} = -k^{\mathrm{on}} \left(c_{\mathrm{A}} c_{\mathrm{B}} - \frac{c_{\mathrm{A}}^{\mathrm{eq}} c_{\mathrm{B}}^{\mathrm{eq}}}{c_{\mathrm{C}}^{\mathrm{eq}} c_{\mathrm{D}}^{\mathrm{eq}}} c_{\mathrm{C}} c_{\mathrm{D}} \right). \tag{B.3}$$

As the thermodynamic force for the chemical reaction is the chemical affinity, if I assume the chemical potentials for A,B,C,D as $\mu_{\mathrm{A}}, \mu_{\mathrm{B}}, \mu_{\mathrm{C}}, \mu_{\mathrm{D}}$,respectively, the chemical affinity A is defined as,

$$A = \mu_{\mathrm{A}} + \mu_{\mathrm{B}} - \mu_{\mathrm{C}} - \mu_{\mathrm{D}} \tag{B.4}$$

Here I consider the relationships between the kinetic equations and the chemical affinity.

B.1 Law of mass action

In the case that the reactant is dilute, the chemical potential is expressed as follow

$$\mu_i = k_{\rm B}T \ln c_i + \mu_i^0(P,T) \tag{B.5}$$

where $\mu_i^0(P,T)$ stands for the standard chemical potential in the state of pressure P and temperature T and $k_{\rm B}$ is the Boltzmann constant. The equilibrium state corresponds to $A = 0$. So substituting eqs.B.5 for A,B,C,D into $A = 0$,

$$A = k_{\rm B}T \ln \frac{c_{\rm A}^{\rm eq} c_{\rm B}^{\rm eq}}{c_{\rm C}^{\rm eq} c_{\rm D}^{\rm eq}} + \mu_{\rm A}^0 + \mu_{\rm B}^0 - \mu_{\rm C}^0 - \mu_{\rm D}^0 = 0 \tag{B.6}$$

Then the law of mass action which is expressed by the following relation is derived from eq.B.6.

$$\ln \frac{c_{\rm A}^{\rm eq} c_{\rm B}^{\rm eq}}{c_{\rm C}^{\rm eq} c_{\rm D}^{\rm eq}} = \frac{\mu_{\rm C}^0 + \mu_{\rm D}^0 - \mu_{\rm A}^0 - \mu_{\rm B}^0}{k_{\rm B}T} \equiv K(P,T), \tag{B.7}$$

where $K(P,T)$ is called the equilibrium constant. The law of mass action means that the ratio of reactants and products becomes a constant depending only on the temperature and pressure in the equilibrium state.

B.2 Linear response

From the law of mass action, the chemical affinity is expressed as below,

$$A = k_{\rm B}T \left[\left(\frac{n_{\rm A} n_{\rm B}}{n_{\rm C} n_{\rm D}} \right) \Big/ \left(\frac{n_{\rm A}^{\rm eq} n_{\rm B}^{\rm eq}}{n_{\rm C}^{\rm eq} n_{\rm D}^{\rm eq}} \right) \right]. \tag{B.8}$$

Also this is expressed as below,

$$e^{-A/k_{\rm B}T} = \frac{n_{\rm C} n_{\rm D} n_{\rm A}^{\rm eq} n_{\rm B}^{\rm eq}}{n_{\rm A} n_{\rm B} n_{\rm C}^{\rm eq} n_{\rm D}^{\rm eq}} \tag{B.9}$$

In the case $A/k_{\rm B}T \ll 1$, I expand A in eq. B.9 with the Taylor series at $A/k_{\rm B}T$,

$$e^{-A/k_{\rm B}T} \simeq 1 - \frac{A}{k_{\rm B}T} + \cdots. \tag{B.10}$$

So the monomer concentration of A expressed as below,

$$\frac{dn_{\rm A}}{dt} \simeq -k n_{\rm A} n_{\rm B} \frac{A}{k_{\rm B}T}. \tag{B.11}$$

Then the linear response coefficient L is as following,

$$L = \frac{k n_{\rm A} n_{rmB}}{k_{\rm B}T} \tag{B.12}$$

Bibliography

[1] T. Horio and H. Hotani, *Nature* **321** 605-607 (1986).

[2] Y. Harada et al. *Nature* **326**, 805–808 (1987).

[3] L. Cassimeris, N. K. Pryer, and E. D. Salmon *J. Cell Biol.* **107**, 2223–2231 (1988).

[4] T. Funatsu, Y. Harada, M. Tokunaga, K. Saito and T. Yanagida, *Nature* **374**, 555–559 (1995).

[5] I. Fujiwara et al. *Nature Cell Biol.* **4**, 666–673 (2002).

[6] H. Lodish, *et al.* (ed.), *Molecular Cell Biology 4th Edition*, W. H. Freeman and Company, New York (2000).

[7] F. Oosawa and M. Kasai *J. Mol. Biol.* **4**, 10–21 (1962).

[8] M. Matsumoto, S. Saito and I. Ohmine, *Nature* **416**, 409–413 (2002).

[9] M. Tomita et al., *Bioinformatics* **15**, 72–84 (1999).

[10] J. Howard, *Mechanics of Motor Proteins and the Cytoskeleton* (Sinauer Associates, Inc., Massachusetts, 2001).

[11] H. Wang and G Oster, *Nature* **396**, 279 - 282 (1998).

[12] L. Amos and A. Klug, *J. Cell Sci.* **14**, 523–549 (1974).

[13] P. B. Moore, H. E. Huxley, and D. J. DeRosier, *J. Mol. Biol.* **50**, 279–295 (1970).

[14] C. A. D. Parry, and P. M. Steinert, *Intermediate Filament Structure.*, Springer-Verlag, New York (1995).

[15] E. Nogales, S. G. Wolf and K. H. Dowing, *Nature* **391**, 199–203 (1998).

[16] W. Kabsch, H. G. Mannherz, D. Suck, E. F. Pai, and K. C. Holmes, *Nature* **347**, 37–44 (1990).

[17] J.-M. Lehn, *Supramolecular chemistry : concepts and perspectives* (John Wiley & Sons, New York, 1995).

[18] Y. L. Wang, *J. Cell Biol.* **101**, 597–602 (1985).

[19] A. Wegner, *J. Mol. Biol.* **108**, 139–150 (1967).

[20] T. J. Mitchison, *J. Cell Biol.* **109**, 637–652 (1989).

[21] R. L. Margolis, and L. Wilson, *Cell* **13**, 1–8 (1978).

[22] T.J. Mitchison and M.W. Kirschner, *Nature* **391** 237–242 (1984).

[23] E. M. Lifshitz and L. P. Pitaevskii, *Physical kinetics* - Course of theoretical physics vol.10 (Pergamon, Oxford, 1981).

[24] J.D. van der Waals, "Over de continüiteit van den gas- en vloeistoftoestand" *Thesis*, University of Leiden (1873) (On the continuity of gas and fluid states).

[25] M. Dogterom and S. Leibler, *Phys. Rev. Let.* **70**, 1347–1350 (1993).

[26] T. Furuta and K. Ebina, "A lattice model for a linear polymer oscillation" in AIP CP519 *Statistical Physics*, M. Tokuyama, H. E. Stanley, Eds., (American Institute of Physics, New York, 2000) pp.516-518.

[27] T. Furuta and K. Ebina, *Physica A* **314**, 163–169 (2002).

[28] T. Furuta and K. Ebina, "Analysis of the growth and shrinkage velocity of a single polymer: a lattice polymerization model in two dimensions" in *Similarity in diversity*, D. L. Morabito and Y. Okamura, Eds., (Nova Science, New York, 2003) pp.223–228.

[29] H. Gould and J. Tobochnik, *An introduction to computer simulation methods* (Addison-Wesley, New York, 1988).

[30] J. Hoshen and R. Kopelman, *Phys. Rev.* **B14**, 3438–3445 (1976).

[31] T. A. Witten and L. M. Sander, *Phys. Rev. Lett.* **47**, 1400–1403 (1981).

[32] E. Boeker and R. van Grondelle, *Environmental Physics* (John Wiley & sons, ltd, New York, 1999).

[33] E. M. Lifshitz and L. P. Pitaevskii, *Statistical physics* - Course of theoretical physics vol.5 (Pergamon, Oxford, 1980).